

Ising Spectroscopy I: Mesons at $T < T_c$

P. Fonseca and A. Zamolodchikov^{1,2}

¹NHETC, Department of Physics and Astronomy
Rutgers University
Piscataway, NJ 08855-0849, USA

²L.D. Landau Institute for Theoretical Physics
Chernogolovka, 142432, Russia

Abstract

This paper is our progress report on the project “Ising spectroscopy”, devoted to a systematic study of the mass spectrum of particles in the 2D Ising Field Theory in a magnetic field. Here we address the low-temperature regime, and develop a quantitative approach based on the idea (originally due to McCoy and Wu) of particles being the “mesons”, consisting predominantly of two quarks confined by a long-range force. Systematic implementation of this idea leads to a version of the Bethe-Salpeter equation, which yields infinite sequence of meson masses. The Bethe-Salpeter spectrum becomes exact in the limit when the magnetic field is small, and we develop the corresponding weak-coupling expansions of the meson masses. The Bethe-Salpeter equation ignores the contributions from the multi-quark components of the meson’s states, but we discuss how it can be improved by treating these components perturbatively, and in particular by incorporating the radiative corrections to the quark mass and the coupling parameter (the “string tension”). The approach fails to properly treat the mesons above the stability threshold, where they are expected to become resonance states, but it is shown to yield a very good approximation for the masses of all stable particles, at all real values of the IFT parameters in the low-temperature regime. We briefly discuss how the Bethe-Salpeter approximation can be used to address the case of complex parameters, which was the main motivation of this work.

1 Introduction

The Ising Field Theory (IFT) is the quantum field theory in two dimensions which emerges in the scaling limit of the Ising model (or any other system from the same universality class) near its critical point. The RG fixed point associated with the Ising criticality is the $c = 1/2$ Minimal Conformal Field Theory (see e.g. [1, 2]) which has two nontrivial relevant operators. Therefore the IFT is understood as the Minimal CFT perturbed by the two relevant operators, as described by the Euclidean Action

$$\mathcal{A}_{\text{IFT}} = \mathcal{A}_{c=1/2 \text{ CFT}} + \tau \int \varepsilon(x) d^2x + h \int \sigma(x) d^2x , \quad (1.1)$$

where the fields $\varepsilon(x)$ (“energy density”) and $\sigma(x)$ (“spin density”) have conformal dimensions $(\frac{1}{2}, \frac{1}{2})$ and $(\frac{1}{16}, \frac{1}{16})$, respectively¹. The parameters τ and h are scaled deviations of the temperature T and the external magnetic field H of the Ising model from the critical values, i.e. $\tau \simeq T_c - T$ and $h \simeq H$ in the limit $T_c - T \rightarrow 0, H \rightarrow 0$. In what follows we refer to h as the magnetic field. It is assumed here that the definition of $\varepsilon(x)$ is such that the domain $\tau > 0$ corresponds to the low-temperature (ordered) phase of the model. The parameters τ and h are dimensionfull, $\tau \sim [length]^{-1}$ and $h \sim [length]^{-\frac{15}{8}}$. Therefore the physics of IFT essentially depends on a single dimensionless scaling parameter, which we define as²

$$\eta = \frac{m}{|h|^{\frac{8}{15}}} \equiv 2\pi \frac{\tau}{|h|^{\frac{8}{15}}} , \quad (1.2)$$

where we have also introduced the notation $m = 2\pi\tau$ which is extensively used below.

Besides its value as the model of near-critical statistical mechanics, the IFT appears to be rich a model of two-dimensional particle theory. It was argued in the pioneering work of McCoy and Wu [3] that as one changes η from $-\infty$ to $+\infty$, the spectrum of stable particles undergoes evolution from a single particle to an infinite tower of “mesons” formed by weakly confined “quarks”. This scenario was subsequently confirmed by exact [5] and numerical [4, 6] results, where some quantitative details were added.

¹Here we assume conventional normalization of the fields, such that

$$\langle \varepsilon(x)\varepsilon(0) \rangle \rightarrow |x|^{-2} \quad \text{and} \quad \langle \sigma(x)\sigma(0) \rangle \rightarrow |x|^{-\frac{1}{4}} \quad \text{as } x \rightarrow 0 .$$

This condition fixes the normalizations of the couplings τ and h .

²This is the same definition of η as was used in [4, 22]; note that it differs from definition in Refs. [16, 29, 30].

The IFT admits an exact solution in few special cases. First, at zero magnetic field, i.e. at $\eta = \pm\infty$, the IFT is well-known to be the theory of free Majorana fermions (see e.g. [1, 7]) of mass $|m|$. Second, the IFT is shown to be integrable at $m = 0$ and $h \neq 0$ (i.e. at $\eta = 0$) [5]. In the last case, the associated particle theory involves eight stable particles whose scatterings are described by certain factorizable S-matrix. Finally, if one admits complex values of the parameters in (1.1), yet another integrable theory is attributed to the vicinity of the point(s) where h takes special pure-imaginary value $h = \pm i(0.1893\dots)m^{\frac{15}{8}}$. This point is the Yang-Lee edge singularity [8]. In the vicinity of this point one of the particles of the theory becomes light, and its dynamics is described by the integrable Yang-Lee field theory [9–11]. At present there are no indication that IFT (1.1) might be integrable at any other values of the parameters, real or complex.

This paper is our progress report on (a part of) the program “Ising spectroscopy”. The program is about the detailed study of the mass spectrum of the IFT at all values of the scaling parameter (with the emphasis on the analytic properties of the masses as the functions of η), using perturbative expansions around the integrable points, combined with numerical methods. There are several motivations for investing effort in this program. For one, the IFT appears in some ways the most basic unitary quantum field theory in two dimensions. The Ising fixed point is the lowest (in terms of the central charge) nontrivial unitary CFT in 2D [2], and the theory (1.1) corresponds to generic RG flow which originates at this point. Also, the IFT is a playground for studying many phenomena common in QFT, like quark confinement, resonance states, first order phase transition and associated “false” vacuum state, etc.

In this paper we discuss the mass spectrum of the IFT at real h and m , in the low-temperature (low-T) domain $m > 0$, i.e. at real $\eta > 0$. Let us remark here that at $h \neq 0$ distinction between the low-T and high-T ($\eta < 0$) regimes is fuzzy, and to a large extent artificial. Physical quantities like the particle masses pass through the point $\eta = 0$ continuously (in fact, analytically). However, although continuously related, the two regimes call for an emphasis on different phenomena, and often require different theoretical treatment. Therefore the distinction is conventional in the literature on the subject, and we will usually hold to it here and in forthcoming reports on our program.

According to McCoy-Wu scenario, at $\eta < \infty$ the free fermions of the $h = 0$ theory (the “quarks”) become confined in “mesons”. The spectrum of the mesons is dense at large η . As η decreases, the heavier mesons become unstable against decay into the lighter ones, and successively disappear from the spectrum of stable particles, typically becoming resonances. As η approaches zero, there are only three stable mesons (and many resonances) left (see [4]), and at $\eta = 0$ some of the resonances

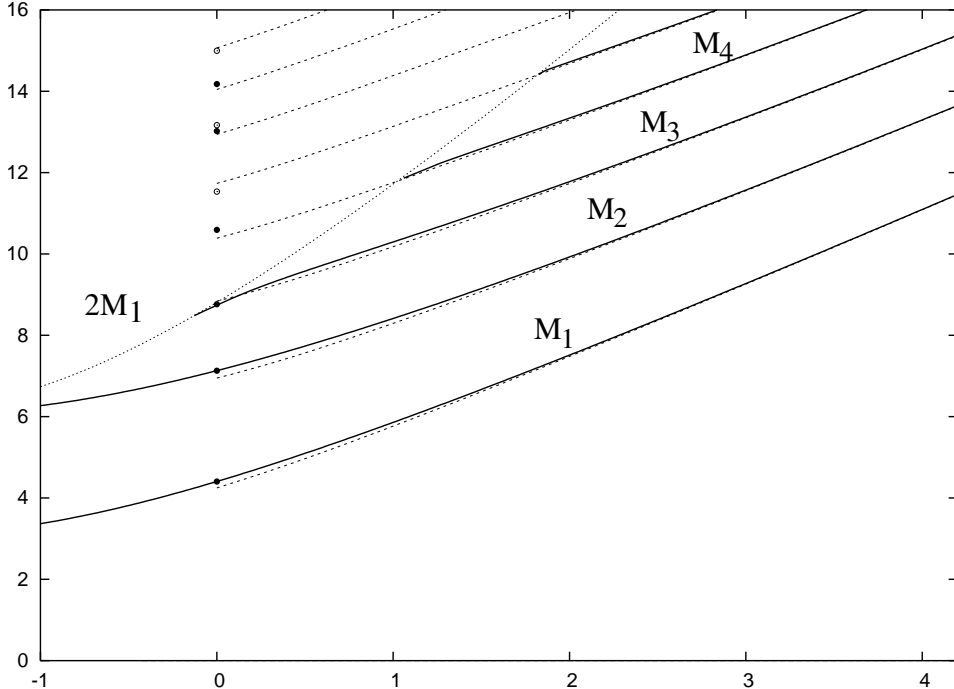


Figure 1: The mass spectrum $M_n(\eta)$ of IFT particles at positive (and some negative) η . The solid lines represent numerical data obtained using the TFFSA. The dotted line shows the stability threshold $2M_1$; after crossing this line the particles become unstable, and their masses (not shown) develop imaginary parts. The exception is the point $\eta = 0$, where there are eight stable particles, whose masses are indicated by bullets \bullet . The dashed lines show the masses obtained from the Bethe-Salpeter equation (4.8), with the renormalized string tension f defined as in Eq.(8.3) (see Section 8 for explanations). The circles \circ indicate positions of the higher thresholds $M_1 + M_2$, $M_1 + M_3$, etc, at $\eta = 0$.

regain stability (the phenomenon related to integrability of the IFT at $\eta = 0$), so there are exactly eight stable particles present³. Very accurate numerical data for the particle masses M_n at all η can be obtained using the “Truncated Free Fermion Space Approach” (TFFSA)⁴; the results for positive η are shown in Fig.1. The form

³The process of depletion of the spectrum continues when η crosses to the negative values, until below a certain point ($\eta < \eta_2 \approx -2.09$, see [4]) there is only one stable particle left. At $\eta \rightarrow -\infty$ all interactions disappear and this particle becomes a free one, in accord with the IFT at zero h being a theory of free fermions. We have much more to say about detailed structure of the spectrum in this domain, but will defer this discussion to another paper.

⁴The TFFSA is a modification of the “Truncated Conformal Space Approach” (TCSA) of Ref. [12], particularly suited for the IFT, see Ref. [4] for details.

of the mass spectrum at sufficiently large η is consistent with the McCoy-Wu idea of the particles being composed of two weakly confined quarks. This idea allows one to develop the weak-coupling (large- η) expansions of the masses $M_n(\eta)$. The leading term was first obtained in the original paper [3], and several further terms added in Ref. [4]. On the other hand, for highly excited mesons the semiclassical approximation applies, and the corresponding expansion was recently derived by Rutkevich [13]⁵.

In this work we develop a more systematic approach based on the two-quark approximation. In Sections 3 and 4 we derive the Bethe-Salpeter (BS) equation, i.e. the relativistic two-quark bound state equation for the IFT mesons. It is not exactly a textbook exercise because no covariant perturbation theory for the IFT is available, and one has to do with the ordinary non-covariant approach. In Section 4 we argue that the Lorentz covariance is restored by adding certain corrections to the quark self-energy, which technically come from the multi-quark sectors. The resulting BS equation (Eq.(4.8)) is very similar to the bound-state equation previously obtained by 't Hooft for the two-dimensional model of multicolor QCD [14], which is not surprising because the physics is similar. The two-quark approximation can be improved by taking the multi-quark sectors into account perturbatively. In Section 6 we discuss the role of the multi-quark corrections, in particular the effects of the renormalizations of basic parameters - the quark mass and “string tension” - due to the multi-quark effects. In Sections 7 and 8 we find the spectrum of the BS equation numerically, and make a tentative comparison with the TFFSA data. If the renormalization of the string tension is taken into account, the BS spectrum reproduces the actual masses rather accurately at all positive η , as is shown in Fig.1. The actual masses $M_n(\eta)$ exhibit a subtle behavior⁶ when they approach the

⁵We have worked out the semiclassical expansion independently, before [13] appeared. Our approach is described in the Section 5 below. We would like to stress that beyond the leading order our result (5.25) differs from the corresponding term found in [13]. The discrepancy can be traced to the corrections to the quark self-energy, which we believe are properly taken into account in the Bethe-Salpeter equation (4.8), but are missing in the treatment in [13].

⁶The near-threshold behavior of the meson masses $M_n(\eta)$ deserves a separate discussion. Preliminary analysis (which will be reported elsewhere) shows the following general pattern. The n -th meson exists as a stable particle while η exceeds certain threshold value, $\eta > \eta_n$, in which domain $M_n(\eta)$ remains below $2M_1(\eta)$. At $\eta = \eta_n$ the graph of $M_n(\eta)$ touches the curve $2M_1(\eta)$, so that $2M_1(\eta) - M_n(\eta) \sim (\eta_n - \eta)^2$ as $\eta \rightarrow \eta_n$. Correspondingly, the analytic continuation of $M_n(\eta)$ to η immediately below η_n remains real, although no stable particle with this mass exists at $\eta < \eta_n$ (the situation known as the “virtual level”, see e.g. [15], §128). By further decreasing the value of η one reaches singularity of the function $M_n(\eta)$ (typically a square-root branching point) at $\eta = \hat{\eta}_n < \eta_n$, and below $\hat{\eta}_n$ the mass $M_n(\eta)$ develops an imaginary part, so that the n -th meson reemerges as a resonance state. This pattern seems to hold for all M_n with $n \geq 3$. Our preliminary estimates of the thresholds are $\eta_2 \approx -2.06$, $\eta_3 \approx -0.136$, $\eta_4 \approx 1.0$, while $\hat{\eta}_3 \approx -0.515$, and the higher $\hat{\eta}_n$ are very close to η_n .

“stability threshold” $2M_1$ (it is visible in Fig.1 for the mass M_3 , and less prominently for M_4 and M_5), the feature certainly driven by the multi-quark components of the meson states. The Bethe-Salpeter approximation does not capture these subtleties. Also, the BS masses remain real above the stability threshold, while the actual IFT particles in this domain generally become unstable, and their masses develop imaginary parts. Although in this paper we do not discuss the resonance part of the IFT spectrum in any detail (we plan to address this important subject separately; some results on the IFT resonances can be found Ref’s [6, 16]), let us note that the pattern shown in Fig.1 suggests that when η goes to zero some of the the IFT resonances turn into the particles of the corresponding integrable theory, while others become weakly coupled bound states of those, with the binding energy $\sim \eta^2$. For instance,

$$M_5(\eta) = M_1(\eta) + M_2(\eta) + O(\eta^2) \quad \text{as } \eta \rightarrow 0. \quad (1.3)$$

This is one of many interesting phenomena which the IFT spectrum appears to exhibit; it provides illustration of its remarkable richness, and gives us additional motivation for its systematic study.

2 Ising quarks and Ising mesons

At $h = 0$, and in the low-temperature phase $m > 0$, the spin-reversal symmetry of the IFT is spontaneously broken, and the theory has two degenerate ground states differing by the sign of the spontaneous magnetization

$$\langle \sigma(x) \rangle_{\pm} = \pm \bar{\sigma}, \quad (2.1)$$

where $\bar{\sigma}$ is a constant whose exact value is [17]

$$\bar{\sigma} = |m|^{\frac{1}{8}} \bar{s}, \quad \bar{s} = 2^{1/12} e^{-\frac{3}{2} \zeta'(-1)} = 1.35783834170660... \quad (2.2)$$

At the same time, as was mentioned in the Introduction, at $h = 0$ the IFT (1.1) reduces to the theory of free Majorana fermions of the mass m . These free fermions are identified with the domain walls separating the spatial domains of positive and negative magnetization. Such interpretation makes it obvious that adding the interaction term $h \int \sigma(x) d^2x$ with small h ($h \ll m^{\frac{15}{8}}$) to the free theory generates confining force between the domain walls, with the “string tension” $2\bar{\sigma}h$. Due to this effect, the stable particles appear as the “mesons”, i.e. the bound states of two “quarks” ⁷.

⁷The gauge group associated with this confining interaction is Z_2 (the Ising model with magnetic field is known to be dual to the Z_2 gauge theory, see e.g. [1]), hence the quarks and the antiquarks are identical.

The above picture alone allows one to give some quantitative description of the masses M_n , $n = 1, 2, 3, \dots$ of the mesons in the limit $\eta \rightarrow +\infty$. Indeed, the Hamiltonian of two particles interacting via the confining force is

$$H = \omega(p_1) + \omega(p_2) + 2\bar{\sigma}h |x_1 - x_2| , \quad (2.3)$$

where x_1, x_2 and p_1, p_2 are the coordinates and the momenta of the quarks, and

$$\omega(p) = \sqrt{m^2 + p^2} . \quad (2.4)$$

For the lower part of the meson spectrum (M_n with n fixed) the non-relativistic approximation $\omega(p) \approx m + p^2/2m$ applies, and the problem reduces to finding energy levels of the Hamiltonian $p^2/m + 2\bar{\sigma}h|x|$. Since the quarks are fermions, only odd levels are relevant, and one finds

$$M_n - 2m \rightarrow (2\bar{\sigma}h)^{\frac{2}{3}} z_n \quad \text{as } h \rightarrow 0 \quad (2.5)$$

where $z_n, n = 1, 2, \dots$ are consecutive zeros of the function $\text{Au}(-z)$. This result was first obtained by McCoy and Wu [3] in their analysis of the spin-spin correlation function. For higher mesons (M_n with $n \sim m^2/\bar{\sigma}h$) the semiclassical approximation is more suitable. Classical trajectories of the system (??) are periodically repeated cycles in which, during the time between two collisions, the quarks move under constant acceleration directed towards each other. It is convenient to parametrize the time t as $(t - t_0) = R \sinh \beta$, where t_0 is suitable reference time, and $R = m/(2\bar{\sigma}h)$. The parameter β has a simple meaning: $+\beta$ and $-\beta$ are the rapidity of the two quarks in the center-of-mass frame. In this frame, the classical trajectory within each cycle is given by the equations (up to permutation of the quarks)

$$p \equiv \frac{(p_1 - p_2)}{2} = -m \sinh \beta , \quad x \equiv x_1 - x_2 = 2R (\cosh \vartheta - \cosh \beta) \quad (2.6)$$

for $-\vartheta < \beta < \vartheta$, where ϑ is positive parameter characterizing the classical trajectory. At $\beta = \pm\vartheta$ the separation between the quarks vanishes, hence the mass (i.e. the center-of-mass energy (??)) associated with the trajectory is $M = 2m \cosh \vartheta$. The reduced action per cycle is

$$\int_{\text{cycle}} p dx = 2mR \int_{-\vartheta}^{\vartheta} \sinh^2 \beta d\beta = \frac{\sinh 2\vartheta - 2\vartheta}{\lambda} ; \quad (2.7)$$

here and below we use the notation λ for the dimensionless ratio

$$\lambda = \frac{2\bar{\sigma}h}{m^2} . \quad (2.8)$$

If one first treats the quarks as distinguishable particles, the full period consists of two cycles, so that the reduced action per period is twice the value of (2.7), so that the Bohr-Sommerfeld quantization condition reads $2 \int_{\text{cycle}} p dx = 2\pi(N + 1/2)$, where the integers N must be taken to be odd, $N = 2n - 1$, to reclaim the fermionic nature of the quarks. The quantization condition then takes the form

$$\frac{\sinh 2\vartheta_n - 2\vartheta_n}{\lambda} = 2\pi (n - 1/4) , \quad n = 1, 2, 3, \dots \quad (2.9)$$

leading to the WKB mass spectrum of the mesons,

$$M_n = 2m \cosh \vartheta_n . \quad (2.10)$$

3 The two-quark approximation

The idea of the Ising particles being predominantly two-quark composites allows one to develop somewhat a more systematic theory of mesons, in particular to develop a weak-coupling expansions for their masses M_n . One starts with the free-fermion theory at $h = 0$, and introduces the creation and annihilation operators \mathbf{a}_p^\dagger and \mathbf{a}_p (where p denotes the spatial momentum of the particle), subject to the canonical anticommutators $\{\mathbf{a}_p, \mathbf{a}_q^\dagger\} = 2\pi \delta(p - q)$. Below we will use the notation

$$| p_1, p_2, \dots, p_n \rangle \equiv \mathbf{a}_{p_1}^\dagger \mathbf{a}_{p_2}^\dagger \dots \mathbf{a}_{p_n}^\dagger | 0 \rangle \quad (3.1)$$

for the n -particle states.

The $h = 0$ theory is described by the free Hamiltonian

$$\mathbf{H}_0 = E_0 + \int_{-\infty}^{\infty} \omega(p) \mathbf{a}_p^\dagger \mathbf{a}_p \frac{dp}{2\pi} , \quad (3.2)$$

where $\omega(p)$ is the relativistic energy (2.4), and E_0 is the ground-state energy. The interaction is generated by adding the term associated with the last term in the action (1.1),

$$\mathbf{H} = \mathbf{H}_0 + h \int_{-\infty}^{\infty} \sigma(x) dx , \quad (3.3)$$

where x is the spatial coordinate, and $\sigma(x) = \sigma(x, t)|_{t=0}$. The operator $\sigma(x)$ can not be expressed through the fermions in a local way (see e.g. [1]), but its matrix elements between the states with any number of the fermions are known explicitly [18]. Here we will only need the $2 \rightarrow 2$ matrix element

$$\langle p_1, p_2 | \sigma(0) | q_1, q_2 \rangle = 4\bar{\sigma} \mathcal{G}(p_1, p_2 | q_1, q_2) , \quad (3.4)$$

where

$$\mathcal{G}(p_1, p_2 | q_1, q_2) = \frac{(1/4)}{\sqrt{\omega(p_1)\omega(p_2)\omega(q_1)\omega(q_2)}} \left[\frac{\omega(p_1) + \omega(q_1)}{p_1 - q_1} \frac{\omega(p_2) + \omega(q_2)}{p_2 - q_2} - \frac{\omega(p_1) + \omega(q_2)}{p_1 - q_2} \frac{\omega(p_2) + \omega(q_1)}{p_2 - q_1} + \frac{p_1 - p_2}{\omega(p_1) + \omega(p_2)} \frac{q_1 - q_2}{\omega(q_1) + \omega(q_2)} \right] \quad (3.5)$$

One looks for the eigenstates of the Hamiltonian (3.3) of the form

$$|\Psi\rangle = |\Psi^{(2)}\rangle + |\Psi^{(4)}\rangle + |\Psi^{(6)}\rangle + \dots \quad (3.6)$$

where

$$|\Psi^{(2)}\rangle = \frac{1}{2} \int_{-\infty}^{\infty} \frac{dp_1}{2\pi} \frac{dp_2}{2\pi} \Psi(p_1, p_2) |p_1, p_2\rangle \quad (3.7)$$

is the two-quark component, and further terms in (3.6) represent contributions from the multi-quark (i.e. the four-quark, six-quark, etc) sectors. The two-quark approximation is developed under the assumption that (3.7) is the dominating component of the meson state. It is certainly valid at sufficiently weak coupling, when the parameter λ is small, but we will see that it provides meaningful description of the spectrum even at very large values of this parameter. Anyway, the two-quark approximation can be improved by taking the multi-quark components in (3.6) into account perturbatively (see Sect.6).

The two-quark component is completely characterized by the “meson wavefunction” $\Psi(p_1, p_2)$ in (3.7). By the definition (3.7) the wave function is antisymmetric, $\Psi(p_1, p_2) = -\Psi(p_2, p_1)$. If the multi-quark components in (3.6) are neglected, the eigenvalue problem $(\mathbf{H} - E) |\Psi_P\rangle = 0$ reduces to the integral equation

$$[\varepsilon(p_1) + \varepsilon(p_2) - \Delta E] \Psi(p_1, p_2) = f_0 \int_{-\infty}^{\infty} 2\pi \delta(p_1 + p_2 - q_1 - q_2) \mathcal{G}(p_1, p_2 | q_1, q_2) \Psi(q_1, q_2) \frac{dq_1}{2\pi} \frac{dq_2}{2\pi} \quad (3.8)$$

where at this point $\varepsilon(p)$ stands for the free quark energy $\varepsilon(p) = \omega(p) = \sqrt{m^2 + p^2}$; we introduce this new notation here in preparation to the discussion in Sect.4 below, where $\varepsilon(p)$ will become the “dressed” quark energy. In (3.8) $\Delta E = E - E_{\text{vac}}$ is the energy above the ground state, and

$$f_0 = 2\bar{\sigma} h = m^2 \lambda \quad (3.9)$$

is the “string tension”. In fact we will refer to the parameter f_0 , Eq.(3.9), as the “bare” string tension, as opposed to “dressed”, or “effective” string tension f which

will replace f_0 when radiative corrections (originating from the multi-quark components in (3.6)) are taken into account, as will be discussed in greater details in Sect.6. The kernel \mathcal{G} in the right-hand side is the matrix element (3.5). The kernel is singular, and the r.h.s. of (3.8) involves the principal value of the singular integral. For the meson state with the momentum P one takes the wave function of the form

$$\Psi(p_1, p_2) = (2\pi) \delta(p_1 + p_2 - P) \Psi_P(p_1 - P/2) \quad (3.10)$$

with antisymmetric $\Psi_P(p) = -\Psi_P(-p)$. Then the equation (3.8) takes the form

$$[\varepsilon(P/2 - p) + \varepsilon(P/2 + p) - \Delta E] \Psi_P(p) = f_0 \int_{-\infty}^{\infty} G_P(p|q) \Psi_P(q) \frac{dq}{2\pi}, \quad (3.11)$$

where the kernel $G_P(p|q)$ is the function (3.5) evaluated at $p_1 + p_2 = q_1 + q_2 = P$,

$$G_P(p|q) = \mathcal{G}\left(\frac{P}{2} + p, \frac{P}{2} - p \middle| \frac{P}{2} + q, \frac{P}{2} - q\right). \quad (3.12)$$

The meson wave-function $\Psi_P(p)$ is assumed to be normalizable ⁸,

$$\|\Psi_P\|^2 \equiv \frac{1}{2\Delta E} \int_{-\infty}^{\infty} |\Psi_P(p)|^2 \frac{dp}{2\pi} < \infty, \quad (3.13)$$

and the equation (3.11) is understood as the eigenvalue problem for the meson energy ΔE .

Observe that the kernel $G_P(p|q)$ in (3.11) has the second-order poles at $q = \pm p$, with the residues 1. More precisely, one can check that

$$G_P(p|q) = \frac{1}{(p-q)^2} - \frac{1}{(p+q)^2} + G_P^{(\text{reg})}(p|q), \quad (3.14)$$

where the last term is regular when both p and q take real values. Therefore the principal value integral in the r.h.s. of (3.11) has the same effect as the linear potential in (2.3), provided the separation between the quarks is large enough, $m|x_1 - x_2| \gg 1$. The short-range interaction described by the regular term $G_P^{(\text{reg})}(p|q)$ is what makes (3.11) different from the simple-minded Eq.(2.3).

The integral equation (3.11) is the result of straightforward application of the idea of the meson being the two-quark construct. However, it is well known that in an

⁸More precisely, the states (3.7) are assumed to be δ -normalizable in terms of the meson momentum P . Since

$$\langle \Psi_P | \Psi_{P'} \rangle = 2\pi \Delta E \delta(P - P') \|\Psi_P\|^2$$

this implies the Eq.(3.13). The factor ΔE is inserted here in anticipation of relativistic normalization of the meson states.

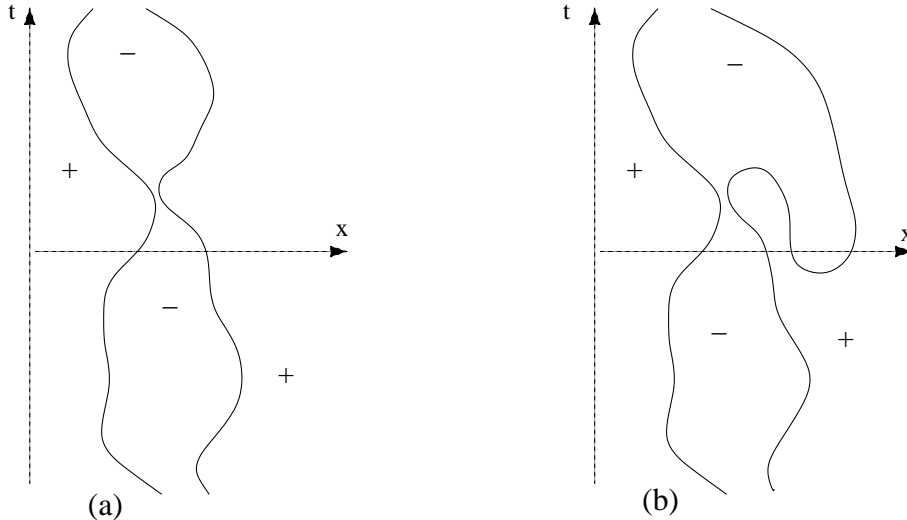


Figure 2: Possible world lines of quarks in a meson. (a) Both quarks propagate forward in time. (b) Creation and annihilation of virtual pairs leads to the presence of more than two quarks in the intermediate state.

interacting theory neglecting the multi-quark components of the state (3.6) generally violates Lorentz invariance. This is because in a relativistic theory the quarks must be allowed to move occasionally backward in time, the possibility depicted in Fig.2 but obviously neglected when all the multi-quark terms in (3.6) are discarded. As the result, the equation (3.11) is not Lorentz-invariant, in particular the eigenvalues ΔE are not expected to have correct dependence $\sqrt{M^2 + P^2}$ on the momentum P .

To restore the Lorentz invariance, it is necessary to retain certain contributions from the multi-quark sectors in (3.6), the ones associated with the backward-in-time propagations of the type depicted in the Fig.2b. Adding such contributions would result in the Lorentz invariant version of the two-quark approximation. Analogous problem in perturbative quantum field theory is solved by the Bethe-Salpeter equation (see e.g. [19]). Unfortunately, in the IFT manifestly covariant perturbation theory in \hbar is not available. For that reason, in the next Section we discuss the multi-quark contributions associated with the backward-in-time propagation of the quarks. These contributions are described as corrections to the dispersion law of the quarks inside the meson. We will argue that these corrections disappear in the limit $P \rightarrow \infty$, and therefore the Lorentz-invariant Bethe-Salpeter equation is essentially the equation (3.11) in the infinite-momentum frame. Similar arguments were previously put forward in the context of the 'tHooft model in [20]

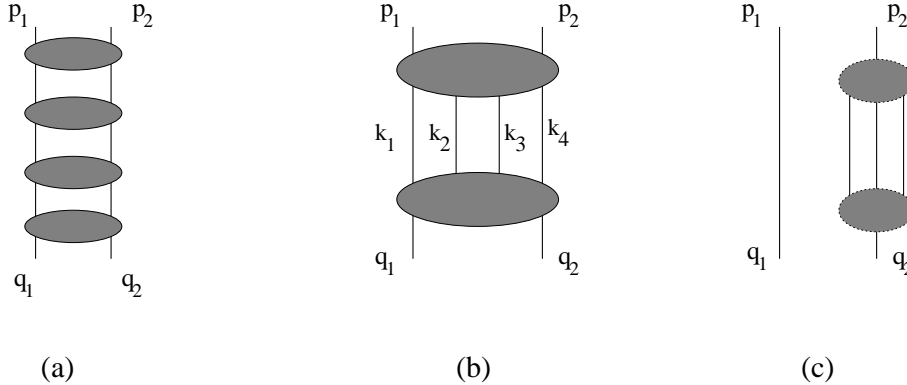


Figure 3: Diagrams of the perturbation theory in h . (a) The “ladder” diagrams. The blobs represent the matrix elements (3.4). These diagrams are summed up by the Eq.(3.11). (b) The diagram with four intermediate quarks. (c) Example of a disconnected part of the diagram in (b).

4 The Bethe-Salpeter equation

As usual, the integral equation (3.11) can be understood as a device for summing up certain class of diagrams of the perturbation theory in h . Here and below we have in mind usual quantum-mechanical perturbation theory (see e.g. [15]), not the covariant Feynman perturbation theory⁹, so that all the intermediate lines in the diagrams below are on-shell. The equation (3.11) takes into account the “ladder” diagrams shown in Fig.3a, where the blobs represent the matrix elements (3.4), with only two quarks involved in the intermediate states. But the Eq.(3.11) neglects all the diagrams with four, six, or more intermediate quarks, like the one shown in the Fig.3b. The blobs in the Fig.3b stand for the matrix elements between the two-quark and four-quark states, and the integration over the intermediate momenta k_1, k_2, k_3, k_4 (subject to the constraint $k_1 + k_2 + k_3 + k_4 = p_1 + p_2 = q_1 + q_2$) is implied. The contribution of the diagram in Fig.3b contains disconnected parts, in which only one of the particles is affected by the interaction, as is depicted by the diagram in Fig.3c. In the disconnected parts like this the momentum conserves separately within each disconnected component, i.e. such diagrams contain two momentum δ -functions. In particular, the contribution of the diagram in Fig.3c to the energy can be written as

$$\left[\begin{array}{c} \text{disconnected} \\ \text{diagram in Fig.3c} \end{array} \right] = (2\pi)^2 \delta(p_1 - q_1) \delta(p_2 - q_2) \Sigma_2^{(3)}(p_2), \quad (4.1)$$

⁹As was already said, manifestly covariant perturbation theory in h is not yet developed. See however calculations in Ref. [21] which seem to be suggestive in this respect.

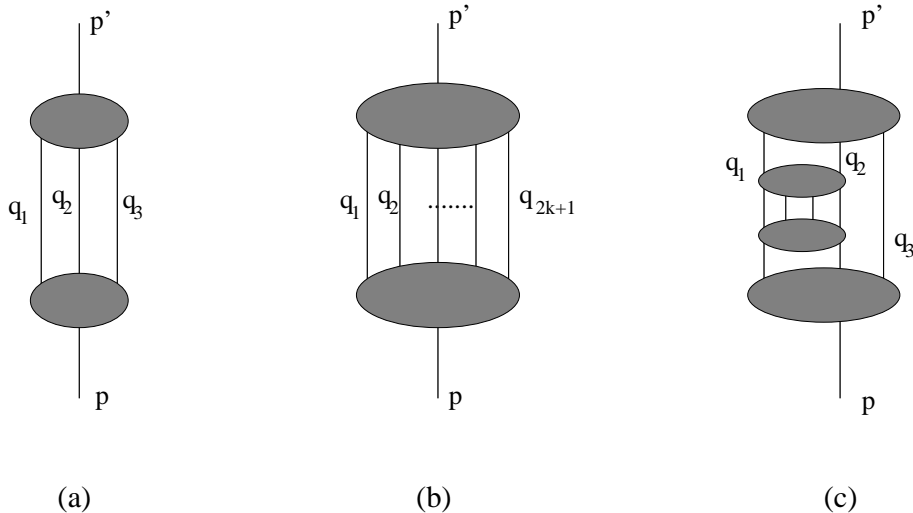


Figure 4: The quark self-energy: (a) The simplest self-energy diagram of the order $\sim h^2$; its contribution $\Sigma_2^{(3)}(p)$ appears in the Eq.(4.1). (b), (c) Examples of more complicated self-energy diagrams.

where $\Sigma_2^{(3)}(p)$ is the self-energy term from the diagram in Fig.4a. Clearly, (4.1) and similar disconnected contributions involving the self-energy diagrams in Fig.4 can be accounted for by replacing the factors $\omega(p) = \sqrt{m^2 + p^2}$ in the left-hand side of the Eq.(3.8) by the dressed quark energy, $\omega(p) \rightarrow \varepsilon(p) = \omega(p) + \Sigma(p)$, where the self-energy correction $\Sigma(p)$ in principle can be determined order by order in the perturbation theory in h . On general grounds, one expects to have two kinds of perturbative contributions to the self-energy. As usual, there are contributions associated with the one-particle irreducible diagrams. These corrections do not modify the relativistic form (2.4) of the momentum dependence of the quark energy, while making corrections to the quark mass m . At this stage we shall ignore the radiative corrections to the quark mass¹⁰, postponing the discussion to Section 6. Here we are more interested in the contributions from the one-particle reducible diagrams. Simplest example of the one-particle reducible diagram is shown in Fig.5b, which can be interpreted as the quark traveling backward in time in between two interaction events. Note that unlike the one-particle reducible diagram with the

¹⁰The leading correction $\sim h^2$ to the quark was determined in Ref. [22] (the result is quoted in Eqs.(6.2), (6.3) below). It may be useful to note that the calculations involve subtracting the one-particle reducible parts (Eqs. (5.10),(5.13), and Fig.3 of Ref. [22]), which are exactly the diagrams Fig.5a and Fig.5b here. The leading correction in (4.4) below comes from adding the diagram in Fig.5b back.

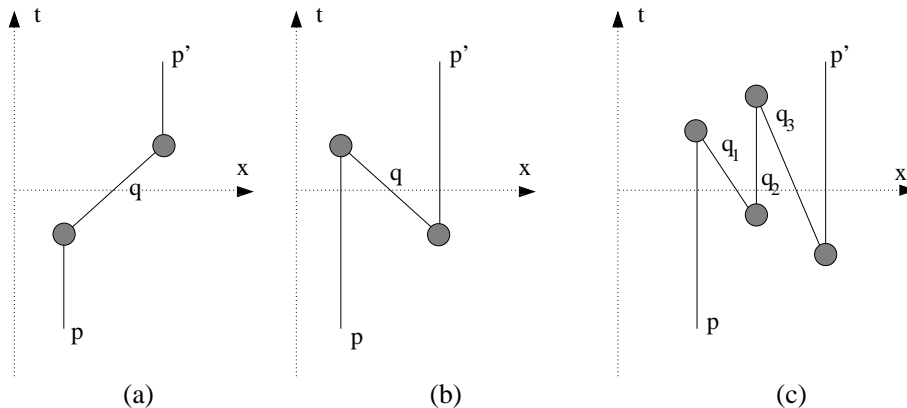


Figure 5: One-particle reducible self-energy diagrams. Parts (a) and (b) show two types of the order h^2 diagrams, with one and three quarks in the intermediate state, respectively. Part (c) shows an example of the higher-order diagrams which contribute to $\varepsilon(p)$.

forward time propagation in Fig.5a, which is already accounted for in the sum of the ladder diagrams in Fig.3a, the diagram in Fig.5b has to be taken into account as separate contribution to $\varepsilon(p)$. The difference between the diagrams Fig.5a and Fig.5b is in the time order of the interaction events; since this distinction may depend on the Lorentz frame, the contribution of the diagram in Fig.5b is not expected to be Lorentz covariant. Similar non-covariant corrections to the quark self-energy arise from the one-particle reducible diagrams of higher orders with the backward-in-time propagation (e.g. the diagram in Fig.5c). The quark energy $\varepsilon(p)$ includes all the one-particle reducible diagrams which are not reproduced by iterations of the equation (3.11) (such are the diagrams in Figs.5b and 5c, but not in Fig.5a).

It is instructive to calculate explicitly the lowest-order correction term in $\varepsilon(p)$, This term comes from the diagram in Fig.5b, which reads

$$- h^2 (2\pi)\delta(p - p') \int_{-\infty}^{\infty} \frac{(2\pi)\delta(p + q) |\langle 0 | \sigma(0) | p, q \rangle|^2 dq}{\omega(p) + \omega(q)} \frac{dq}{2\pi}. \quad (4.2)$$

Performing the trivial integration, and using explicit form [18] of the matrix element

$$\langle 0 | \sigma(0) | p, q \rangle = \frac{i\bar{\sigma}}{\sqrt{\omega(p)\omega(q)}} \frac{p - q}{\omega(p) + \omega(q)} \quad (4.3)$$

one finds

$$\varepsilon(p) = \omega(p) - \frac{\lambda^2}{8} \frac{p^2}{\omega^5(p)} + O(\lambda^4), \quad (4.4)$$

where λ is defined in Eq.(2.8). It is possible to show that this correction in (4.4) is exactly what is needed in order to restore the Lorentz covariance of the spectrum of the equation (3.8), to this order in λ . The calculation supporting this statement is rather involved; we will present it elsewhere.

In principle, the higher order terms in (4.4) can be determined by direct calculation of the corresponding diagrams. It is reasonable to expect that incorporating these terms in $\varepsilon(p)$ will restore the Lorentz covariance of the equation (3.8) order by order in λ^2 (analogous statement for the 't Hooft's model has been proven in Ref. [20]). In particular, with all contributions to $\Sigma(p)$ taken into account, the P -dependence of all the eigenvalues ΔE of (3.8) must assume the relativistic form

$$\Delta E = \sqrt{M^2 + P^2} \quad (4.5)$$

with M interpreted as the meson mass. Let us stress that at the moment we have no proof of this statement beyond the order λ^2 . We intend to come back to this question in the future. In the remaining part of this paper we proceed under this assumption.

Once the assumption is accepted, there is an obvious way to circumvent calculation of $\Sigma(p)$ altogether. Note that the leading term $\sim \lambda^2$ in (4.4) decays fast (as $|p|^{-3}$) when $p \rightarrow \infty$. It is possible to verify that the higher-order terms in (4.4) decay yet faster, so that the asymptotic form

$$\varepsilon(p) = |p| + \frac{m^2}{2|p|} + O\left(\frac{1}{|p|^3}\right) \quad (4.6)$$

is valid to all orders in λ ¹¹. Consider the eigenvalue equation (3.11) and take the limit $P \rightarrow +\infty$. As is shown in Appendix A, in this limit, and under appropriate normalization, the meson wave function $\Psi_P(p)$ remains finite at $2|p|/P < 1$, but vanishes as $1/P^2$ outside this domain. For $2|p|/P < 1$ both sides of the equation (3.11) decay as $1/P$ at large P . Note that this leading term of the $P \rightarrow \infty$ asymptotic is not affected at all by the correction terms in (4.4), since $\Sigma(p)$ decays faster than $1/p$. Balancing the coefficients in front of $1/P$ asymptotic in both sides of (3.11) yields a nontrivial eigenvalue equation for the parameter M^2 in (4.5). This equation is derived in Appendix A. Its most convenient form is obtained by changing to the rapidity variables

$$2p = P \tanh \theta, \quad 2q = P \tanh \theta' \quad (4.7)$$

¹¹Here we ignore all corrections to the quark mass determined by the one-particle irreducible self energy diagrams. Of course, exact asymptotic form of $\varepsilon(p)$ is given by the Eq.(4.6), with m replaced by the "dressed" quark mass m_q .

before sending P to infinity, and introducing the notation $\Psi(\theta)$ for the limit of $\Psi_P(p)$ at $P \rightarrow \infty$. It is

$$\left[m^2 - \frac{M^2}{4 \cosh^2 \theta} \right] \Psi(\theta) = f_0 \int_{-\infty}^{\infty} G(\theta|\theta') \Psi(\theta') \frac{d\theta'}{2\pi}, \quad (4.8)$$

where

$$G(\theta|\theta') = 2 \frac{\cosh(\theta - \theta')}{\sinh^2(\theta - \theta')} + \frac{1}{4} \frac{\sinh \theta}{\cosh^2 \theta} \frac{\sinh \theta'}{\cosh^2 \theta'}. \quad (4.9)$$

We will refer to (4.8) as the Bethe-Salpeter (BS) equation.

Let us make few general remarks on the properties of the BS equation (4.8). First, the wave function $\Psi(\theta)$ should be regarded as a vector in the Hilbert space with the metric

$$||\Psi||^2 = \int_{-\infty}^{\infty} \frac{|\Psi(\theta)|^2}{4 \cosh^2 \theta} \frac{d\theta}{2\pi} \quad (4.10)$$

which is just the metric (3.13) rewritten in terms of the rapidity variable θ , in the limit $P = \infty$. Second, the equation is understood as the eigenvalue problem for the parameter M^2 ,

$$\hat{H}\Psi = M^2\Psi, \quad (4.11)$$

where the operator \hat{H} , defined as

$$\hat{H}\Psi(\theta) = 4 \cosh^2 \theta \left[m^2 \Psi(\theta) - f_0 \int_{-\infty}^{\infty} G(\theta|\theta') \Psi(\theta') \frac{d\theta'}{2\pi} \right], \quad (4.12)$$

is Hermitian with respect to the metric (4.10). Its eigenvalues are real and positive. We will use the notations \widetilde{M}_n^2 with $n = 1, 2, 3, \dots$ for the successive eigenvalues of (4.11) (arranged in the order of increasing magnitude) and $\Psi_n(\theta)$ for the corresponding eigenfunctions. The quantities \widetilde{M}_n provide certain approximations for the actual meson masses, and we reserve the notation M_n for those actual masses.

5 Weak coupling expansions

If the magnetic field h is small, such that $f_0 \ll m^2$, the Bethe-Salpeter equation (4.8) reproduces physics of weakly confined quarks, as described in Sect.2. According to this picture, one expects that in the limit $\lambda \rightarrow 0$ each individual eigenvalue \widetilde{M}_n^2 approaches $4m^2$ from the above, so that the full spectrum $\{\widetilde{M}_n^2\}$ of the equation

(4.11) becomes dense in the segment $[4m^2, \infty)$. Here we develop the weak coupling expansions of the eigenvalues \widetilde{M}_n^2 . The nature of the expansion depends on what part of the spectrum $\{\widetilde{M}_n^2\}$ one is interested in. First, one might be interested in the small- λ expansion of an individual eigenvalue \widetilde{M}_n^2 , with fixed n . Since the kinetic and potential energies of the quarks in any given meson state become small at small λ , we refer to this case as the *low energy expansion*. The equation (2.5) is just the first term of this expansion, and in general the low-energy expansion of \widetilde{M}_n^2 turns to be in fractional powers of λ , namely in the powers of the parameter

$$t = \lambda^{\frac{1}{3}} . \quad (5.1)$$

Second, the behavior of the higher levels \widetilde{M}_n^2 with $n \gtrsim \frac{1}{\lambda}$ may be of interest; in this case one can derive the *semiclassical expansion* extending the Eq.(2.10). This expansion is in integer powers of λ , and the Bohr-Sommerfeld equation (2.10) appears as its leading term, while the higher-order corrections were discussed in [13]. In all cases it is useful to remember that the BS equation itself is an approximation, and therefore starting from certain order (t^9 in the low-energy and correspondingly λ^3 in the semiclassical expansion) both expansions exceed the accuracy of the BS equation (4.8). From these orders on, the coefficients of the weak coupling expansions of the actual masses M_n start to receive contributions associated with the multi-quark components of the meson states¹². In this Section we ignore such corrections, but we will come back to them in Sect.6.

We develop the weak coupling expansions starting from the following approximation for the solution of the equation (4.11) ,

$$\Psi^{(0)}(\theta) = \sinh \theta \int_{-\infty}^{\infty} \frac{e^{\frac{i}{\lambda} S(\beta)} \cosh \beta d\beta}{\sinh(\theta + \beta - i0) \sinh(\theta - \beta + i0)} , \quad (5.2)$$

where

$$S(\beta) = \frac{M^2}{4m^2} \tanh \beta - \beta . \quad (5.3)$$

It is easy to show that $\Psi^{(0)}(\theta)$ is normalizable (with respect to the metric (4.10)) at any value of M^2 . The quality of this approximation is determined by the function $\Delta(\theta|M^2)$ defined as (in what follows we usually suppress the argument M^2)

$$4m^2 \sinh \theta \Delta(\theta) \equiv [\hat{H} - M^2] \Psi_0(\theta) , \quad (5.4)$$

¹²Here we refers to the multi-quark corrections which cannot be absorbed into the renormalizations of the parameters m and f_0 . Corrections to these parameters appear at lower orders; more details are in Section 6.

where \hat{H} is the operator (4.11). By straightforward transformations (which we sketch in the Appendix B) this function can be written as the integral

$$\Delta(\theta) = \int_{-\infty}^{\infty} \left[\frac{M^2}{4m^2 \cosh \beta} + \frac{i\lambda}{8} \frac{\sinh \beta}{\cosh^2 \beta} + \lambda B(\theta|\beta) \right] e^{\frac{i}{\lambda} S(\beta)} d\beta, \quad (5.5)$$

where

$$B(\theta|\beta) = \frac{1}{\pi} \frac{d}{d\beta} \left[\frac{\cosh^2 \theta}{\sinh \theta} \left(\frac{(\theta + \beta)}{\sinh(\theta + \beta)} - \frac{(\theta - \beta)}{\sinh(\theta - \beta)} \right) - \frac{1}{4} \frac{\beta}{\cosh \beta} \right]. \quad (5.6)$$

Note that the terms $\sim \lambda$ in the integrand in (5.5) are sorted out according to their symmetry with respect to $\beta \rightarrow -\beta$.

Next, we develop a small- λ expansion of the integral (5.5). Let us note that the integrand in (5.5) is independent of θ except for the last term $B(\theta|\beta)$ in the brackets there. If the θ dependence could be ignored, it would be possible to turn the whole integral (5.5) to zero by tuning the parameter M^2 to special values, the zeros of the function $\Delta(M^2) \equiv \Delta(\theta|M^2)$; these special values would then determine the eigenvalues \widetilde{M}_n^2 . It turns out that the term $B(\theta|\beta)$ in (5.5) does not contribute to the expansion all the way up to rather high order - up to t^8 of the low-energy expansion and up to λ^2 in the semiclassical expansion - and therefore evaluating first few terms of the weak coupling expansion from (5.5) is very easy. At higher orders the θ -dependence shows up and hence no choice of M^2 can turn the function (5.5) to identical zero. This is well expected - after all (5.2) is an approximate, not exact solution of the Eq.(4.8). Therefore finding the terms of the order λ^3 and higher requires additional ingredients. Let us show how to develop systematic weak coupling expansion of the eigenvalues \widetilde{M}_n^2 to any order¹³.

We start with the trivial observation that any eigenvalue \widetilde{M}_n^2 satisfies the equation

$$C_n(\widetilde{M}^2) = 0, \quad (5.7)$$

where

$$C_n(M^2) = (\Psi_n, [\hat{H} - M^2] \Psi^{(0)}) . \quad (5.8)$$

Here and below the brackets (,) denote the scalar product associated with the metric (4.10) . We also assume the eigenvectors to be orthonormalized, $(\Psi_n, \Psi_k) =$

¹³In the case under consideration the higher order terms have somewhat limited value: as we explain in Section 6 such terms compete with the multi-quark corrections which are generally beyond control of the BS equation (4.8). Here we still do it as a technical exercise, since the method can be applied in other models, notably in the 't Hooft's model of multicolor QCD [14], where very similar Bethe-Salpeter equation (shown as the Eq's (A.6),(A.8) in Appendix A) is exact.

$\delta_{n,k}$. Note that

$$C_n(M^2) = \int \frac{m^2 \sinh \theta \Delta(\theta) \Psi_n(\theta)}{\cosh^2 \theta} \frac{d\theta}{2\pi} . \quad (5.9)$$

At small λ the function $\Psi^{(0)}(\theta)$ provides good approximation for $\Psi_n(\theta)$, and moreover one can find corrections by iterating the equations

$$\Psi_n(\theta) = \frac{1}{(\Psi^{(0)}, \Psi_n)} \left[\Psi^{(0)}(\theta) - \sum_{k \neq n} \frac{C_k(M^2)}{M_k^2 - M^2} \Psi_k(\theta) \right]_{M^2=M_n^2} , \quad (5.10)$$

Then the solution has to be plugged back into (5.8), providing further corrections to the eigenvalues through the Eq.(5.7).

We illustrate this technique by explicit calculations of the first few orders, both in the low-energy and semiclassical expansions.

5.1 Low energy expansion

Assume that the parameter M^2 in (5.5) is close to $4m^2$, so that $M^2 - 4m^2 \lesssim t^2$. Note that any given eigenvalue \widetilde{M}_n^2 enters this domain at sufficiently small λ . When this is the case, the integral (5.5) is dominated by contribution from $\beta \sim t$. It is convenient then to change to a new variable $u = -\beta/t$. We also write $M^2 = 4m^2(1 + zt^2 + O(t^4))$ with some coefficient z to be determined below. In the leading order in t the Eq.(5.5) reduces to the integral defining the Airy function,

$$\Delta(\theta) = t \int_{-\infty}^{\infty} e^{\frac{i}{3}u^3 - izu} du + O(t^3) . \quad (5.11)$$

Hence, it is sufficient to set the parameter $-z$ equal to any zero of the Airy function,

$$\text{Ai}(-z) = 0 , \quad (5.12)$$

to make (5.11) vanish to the leading order in t . This reproduces the equation (2.5). In what follows we use the notation z for a generic solution of the equation (5.12).

More generally, we look for the solutions of (5.7) in the form

$$\frac{\widetilde{M}^2}{4m^2} = 1 + zt^2 + \sum_{k=3}^{\infty} \epsilon_k t^k . \quad (5.13)$$

The integral (5.5) can be evaluated order by order in t . Let us write its expansion as

$$\frac{\Delta(\theta)}{\pi \text{Ai}'(-z)} = D_3(\theta) t^3 + D_4(\theta) t^4 + D_5(\theta) t^5 + \dots . \quad (5.14)$$

A straightforward calculation¹⁴ yields

$$D_3(\theta) = -\epsilon_3, \quad D_4(\theta) = \frac{z^2}{5} - \epsilon_4, \quad D_5(\theta) = -\epsilon_5, \quad \text{etc} \quad (5.15)$$

It turns out that the coefficients $D_k(\theta)$ have no θ -dependence all the way up to $D_8(\theta)$, so that they can be turned to zero by suitable choice of $\epsilon_3, \epsilon_4, \dots, \epsilon_8$, e.g. $\epsilon_3 = 0, \epsilon_4 = z^2/5$, etc. It also turns out that the coefficients ϵ_5 and ϵ_7 obtained in this manner vanish (but higher order odd terms are present in (5.13), see Eq.(5.19) below). Thus we find

$$\frac{\widetilde{M}^2}{4m^2} = 1 + z t^2 + \frac{z^2}{5} t^4 - \left(\frac{3z^3}{175} + \frac{57}{280} \right) t^6 + \left(\frac{23z^4}{7875} + \frac{1543z}{12600} \right) t^8 + \dots \quad (5.16)$$

The first four terms here are identical to the results previously reported in Ref. [4]¹⁵, but the fifth ($\sim t^8$) term is new. Starting with the term $\sim t^9$ the θ -dependent term $B(\theta|\beta)$ in (5.5) becomes relevant, and the coefficients $D_k(\theta)$ with $k \geq 9$ generally have nontrivial dependence on θ . For example

$$D_9(\theta) = \frac{3}{8} B_0(\theta) + \frac{4}{3} B_2(\theta) + 2 B_4(\theta) - \epsilon_9, \quad (5.17)$$

where the functions $B_{2n}(\theta)$ are the coefficients in the expansion

$$B(\theta|\beta) = B_0(\theta) + B_2(\theta) \beta^2 + B_4(\theta) \beta^4 + \dots \quad (5.18)$$

At this order and beyond we have turn to the equation (5.7), and determine the coefficients $\epsilon_9, \epsilon_{10}$, etc from the condition that the integral (5.9) vanishes order by order in t . We do not enter the details of this calculation here, only remark that the integral (5.9) receives the main contribution from the domain $\theta \sim t$, therefore its expansion in t involves the expansions of the coefficients $D_9(\theta), D_{10}(\theta), \dots$ in the powers of θ . Let us quote few more terms of the expansion (5.13),

$$\epsilon_9 = \frac{13}{1120 \pi}, \quad \epsilon_{10} = -\frac{1894 z^5}{3031875} - \frac{23983 z^2}{242550}, \quad \epsilon_{11} = \frac{3313 z}{10080 \pi}. \quad (5.19)$$

¹⁴The calculation involves the integrals

$$\int_{-\infty}^{\infty} (iu)^k e^{\frac{i}{3}u^3 - izu} du \equiv \pi \text{Ai}'(-z) I_k.$$

The factors I_k in the r.h.s. of this equation are easily computed one by one using the recursion

$$I_{k+2} = -z I_k + k I_{k-1} \quad \text{with} \quad I_0 = 0 \quad \text{and} \quad I_1 = 1,$$

where the last two equations follow from Eqs.(5.12) (5.15).

¹⁵Our calculations in Ref. [4] were performed using the Eq.(3.11), with $\varepsilon(p) = \omega(p)$, in the center-of-mass frame $P = 0$. Corrections to $\varepsilon(p)$ contribute to \widetilde{M}_n^2 starting only from the order t^8 ; that is why all terms quoted in [4] are correct.

Quick inspection of (5.16) and (5.19) (as well as the higher order terms) reveals a general structure. The coefficients ϵ_k are polynomials in z , of growing degree. The even coefficients have the form $\epsilon_{2l} = a_l z^l + b_l z^{l-3} + \dots$, while for the odd terms we have $\epsilon_{2l+1} \sim z^{l-4}$. The parameter z becomes large for higher eigenvalues (the Airy zeros grow as $z_n \sim n^{\frac{2}{3}}$). If $t \ll 1$ but $z_n t^2 \sim 1$ or greater, it is useful to sum up the leading terms $\sim (n^{\frac{1}{3}} t)^{2l}$. It is not hard to see that this is exactly what the Bohr-Sommerfeld equation (2.9), (2.10) accomplishes. Then one can try to collect the subleading terms $\sim t^6 (n^{\frac{1}{3}} t)^{2l}$, $\sim t^9 (n^{\frac{1}{3}} t)^{2l}$, etc. This is done by evaluating the higher order terms of the semiclassical expansion, as we discuss next.

5.2 Semiclassical expansion

If $\lambda \ll 1$ and M^2 is not too close to $4m^2$ the integral (5.5) can be evaluated by the stationary phase method. There are two saddle points at $\beta = \pm \vartheta$, where ϑ is a positive parameter defined by the equation

$$M^2 = 4m^2 \cosh^2 \vartheta . \quad (5.20)$$

Correspondingly, the integral can be written as

$$\Delta(\theta) = \Delta_+(\theta) + \Delta_-(\theta) \quad (5.21)$$

where the two terms represents the contribution of the two saddle point $\beta = \pm \vartheta$, respectively. Obviously, $\Delta_-(\theta) = \Delta_+^*(\theta)$, so we can concentrate attention on one of this terms, say $\Delta_+(\theta)$. In the leading approximation only the first term in the square brackets (5.5) contributes, and it has to be evaluated at the saddle point $\beta = \vartheta$. Thus in the leading order $\Delta(\theta)$ is independent of θ , namely

$$\frac{\Delta^{(\text{classical})}(\theta)}{\sqrt{2\pi\lambda \sinh 2\vartheta}} = \cos \left(\frac{\bar{S}(\vartheta)}{\lambda} - \frac{\pi}{4} \right) . \quad (5.22)$$

where

$$\bar{S}(\vartheta) \equiv S(\beta)|_{\beta=\vartheta} = \frac{\sinh 2\vartheta - 2\vartheta}{2} \quad (5.23)$$

($\bar{S}(\vartheta)$ is not the same function as $S(\vartheta)$ because ϑ enters also through (5.20)). Vanishing of (5.22) leads exactly to the quantization condition (2.9).

Corrections to the leading WKB formula can be obtained by developing the standard loop expansions of the integral (5.5) around the saddle points. In the one-loop order the θ -dependent term $B(\theta|\beta)$ still is not too important (its effect is in

bringing in an overall factor $1 + \lambda B(\theta|\vartheta)$ in $\Delta(\theta)$, and $\Delta(\theta)$ still can be turned to identical zero by appropriate adjustment of ϑ . Explicit calculation yields

$$\frac{\Delta_+^{(\text{one-loop})}(\theta)}{\sqrt{2\pi\lambda \sinh 2\vartheta}} \frac{2}{1 + \lambda B(\theta|\vartheta)} = e^{-\frac{i\pi}{4}} e^{\frac{i}{\lambda} \bar{S}(\vartheta)} \left(1 + i\lambda \bar{S}_1(\vartheta) + O(\lambda^2) \right) \quad (5.24)$$

where

$$\bar{S}_1(\vartheta) = -\frac{1}{\sinh 2\vartheta} \left[\frac{5}{24} \frac{1}{\sinh^2 \vartheta} + \frac{1}{4} \frac{1}{\cosh^2 \vartheta} - \frac{1}{12} - \frac{1}{6} \sinh^2 \vartheta \right] \quad (5.25)$$

This leads to the one-loop correction to the quantization condition (2.9),

$$\sinh 2\vartheta_n - 2\vartheta_n = 2\pi\lambda \left(n - 1/4 \right) - \lambda^2 \bar{S}_1(\vartheta_n) - O(\lambda^3) . \quad (5.26)$$

The eigenvalues \widetilde{M}_n^2 are still related to ϑ_n through (5.20), i.e.

$$\widetilde{M}_n^2 = 4m^2 \cosh \vartheta_n \quad (5.27)$$

Let us remark here on the relation to the results of Ref. [13], where the semiclassical expansion to the same order $\sim \lambda^2$ is developed on the basis of the two-quark approximation in the center of mass frame. Our result (5.26) is similar but different from that of [13]. The calculation in [13] ignores the correction $\sim \lambda^2$ to the quark self energy, which is responsible for the Lorentz covariance of our approach. It is easy to check that when the self-energy correction (4.4) is added, the result of [13] becomes identical to (5.26), (5.27) above.

The higher-loop corrections generally leave the Eq.(5.27) unchanged while adding the higher-order terms

$$- \lambda^3 \bar{S}_2(\vartheta_n) - \lambda^4 \bar{S}_3(\vartheta_n) - \dots , \quad (5.28)$$

to the r.h.s. of the Eq.(5.26). Calculation of the coefficients $\bar{S}_2(\vartheta)$, $\bar{S}_3(\vartheta)$, \dots requires (rather straightforward) evaluation of the higher-loop contributions to $\Delta_+(\theta)$ and $\Delta_-(\theta)$ in (5.21). At two loops (and of course at all higher orders as well) $\Delta(\theta)$ acquires an essential dependence on θ , which makes it impossible to turn it to identical zero by an adjustment of ϑ . Just like in our previous analysis of the low-energy expansion, one finds the higher-loop terms in (5.28) from the equation (5.7). Since $\Delta(\theta)$ remains slow-varying function at small λ , the integral in (5.9) is dominated by the stationary-phase points $\theta = \pm \vartheta$ of the function $\Psi_n(\theta)$, and can be evaluated order by order in the associated loop expansion. Thus, at the two-loop level in the mass spectrum calculation, the leading-order stationary-point

calculation of (5.9) is appropriate, therefore the coefficient $\bar{S}_2(\vartheta)$ in (5.28) is found from the equation

$$\Delta^{(\text{two-loop})}(\theta)|_{\theta=\vartheta} = 0 . \quad (5.29)$$

Calculations of yet higher coefficients $S_3(\vartheta)$, $S_4(\vartheta)$, etc involves also iterations of (5.10), along with the higher-loop evaluation of the integral (5.9). We did not perform these straightforward calculations explicitly because, as was mentioned above, all terms beyond λ^2 in (5.26) exceed the accuracy of the BS equation itself - starting from the term λ^3 the expansion of the actual masses M_n receives nontrivial contributions from the multi-quark sectors, and without good control of these corrections the semiclassical analysis at the order λ^3 and beyond does not seem to make much sense.

To conclude this section let us remark that the weak coupling expansions (both the low-energy and semiclassical) of the meson masses are only asymptotic ones. For the expansions of the BS eigenvalues \widetilde{M}_n this fact can be deduced from their analytic structure as the functions of λ : there are infinitely many complex singularities accumulating at the point $\lambda = 0$, as we explain in Sect.9. It is possible to argue that the point $\lambda = 0$ is an essential singularity of the actual masses M_n as well, but this discussion goes beyond the scope of the present paper.

6 Multi-quark corrections

As was already mentioned in the Section 4, the Bethe-Salpeter equation ignores substantial part of the multi-quark contributions to the meson masses. In general, explicit computation of such contributions is a rather difficult task which we do not attempt to perform here. Instead, we briefly discuss the role of the multi-quark corrections, in particular the way they modify the weak-coupling expansions described in the previous Section.

The multi-quark corrections are represented by diagrams with more than two quarks in the intermediate states, like the diagram in Fig.3b. Formally, all such terms can be considered as the higher-order corrections to the kernel in the right-hand side of the equation (3.11),

$$G_P(p|q) \rightarrow \widetilde{G}_P(p|q) = G_P^{(0)}(p|q) + \lambda G_P^{(2)}(p|q) + \lambda^2 G_P^{(3)}(p|q) + \dots , \quad (6.1)$$

where $G_P^{(0)}(p|q) \equiv G_P(p|q)$ is the original kernel (3.12). All terms here are expected to be singular at $p = \pm q$, the singularities being of two types: the delta-function singularities coming from the disconnected diagrams (like the one shown in Fig.3c), and the second-order poles at $p \pm q = 0$ reflecting the long-range character of the interaction in (3.3). Let us discuss first the role of these singular terms.

The delta-function terms were previously discussed in the Section 4. Their role is to modify the quark self-energy $\omega(p) \rightarrow \varepsilon(p)$, and to renormalize the quark mass. The first part is already taken into account in the left-hand side of the equation (3.8), and since the associated one-particle reducible diagrams disappear in the limit $P = \infty$, this part plays no role in the final form of the Bethe-Salpeter equation (4.8). The second part - the quark-mass corrections due to the one-particle irreducible diagrams - can be taken into account if one replaces the parameter m in the Eq.(4.8) by the full “dressed” quark mass m_q . The latter is defined perturbatively, as the sum of all one-particle irreducible self-energy diagrams. By this definition the quark mass is given as the power series

$$m_q^2 = m^2 (1 + a_2 \lambda^2 + a_3 \lambda^3 + \dots) . \quad (6.2)$$

In principle, the coefficients a_k can be determined through well defined calculations within the perturbation theory. However, the problem is rather involved, and at the moment only the first correction term in (6.2) is known exactly [22],

$$a_2 = 0.071010809\dots . \quad (6.3)$$

This and the higher order corrections in (6.2) obviously modify the weak coupling expansions of the meson masses M_n . Thus, in the low-energy expansions of the actual meson masses

$$\frac{M^2}{4m^2} = 1 + \sum_{k=1}^{\infty} \mu_k t^k \quad (6.4)$$

the coefficients μ_k coincide with the corresponding coefficients ϵ_k in (5.13) at $k < 6$, but starting from μ_6 they receive additional contributions due to the quark mass corrections. In particular, at the order t^6 we have

$$\mu_6 = \epsilon_6 + a_2 , \quad (6.5)$$

while the next term $\sim t^7$ receives no correction, so that we still have $\mu_7 = 0$. Yet higher orders are affected by these as well as by other types of the multi-quark corrections, as we explain below. Our present knowledge about the “dressed” quark mass m_q as the function of λ is very limited. No higher order coefficients a_3, a_4, \dots in (6.2) are known even approximately. Moreover, there are no reason to expect the perturbative expansion (6.2) to converge. On a more fundamental level, no clear definition of the dressed quark mass beyond the perturbation theory is available. Therefore, apart from the weak coupling expansions, the quark mass m_q can be treated presently as a phenomenological parameter at best. Taking this point of view we will observe in the Section 8 that the overall radiative correction $\delta m \equiv m_q - m$

is probably very small (no more than $\sim 2 - 3\%$ of the lightest meson mass M_1) at all positive λ .

Next, the even order terms in (6.1) are expected to have the second order poles at $p \pm q = 0$. The pole terms are interpreted as the corrections to the string tension: the “bare” string tension $f_0 = 2\bar{\sigma} h$ in the r.h.s. of the BS equation (4.8) is effectively replaced by the “dressed” one $f = f(h)$. To make it precise, we write

$$f_0 \tilde{G}_P(p|q) = f \mathbb{G}_P(p|q) \quad (6.6)$$

where by definition the kernel \mathbb{G}_P is normalized in such a way that its second order poles have the residues 1, as in (3.14); we can write

$$\mathbb{G}_P(p|q) = G_P(p|q) + \Delta \mathbb{G}_P^{(\text{reg})}(p|q) \quad (6.7)$$

where $G_P(p|q)$ is the original kernel (3.12) which has the standard pole terms (3.14), and the last term is regular at $p = \pm q$ ¹⁶. In this way the coefficient f appears as a power series in λ^2 ,

$$f = f_0 (1 + c_2 \lambda^2 + \dots). \quad (6.8)$$

It is possible to argue that the coefficients c_{2k} here are related in a simple way to the coefficients \tilde{g}_{2k+1} of the weak field expansion

$$\frac{\mathcal{F}_{\text{vac}}}{m^2} - \frac{1}{8\pi} \log m^2 = -\frac{1}{2} \lambda + \tilde{g}_2 \lambda^2 + \tilde{g}_3 \lambda^3 + \tilde{g}_4 \lambda^4 + \dots, \quad (6.9)$$

of the IFT vacuum energy density \mathcal{F}_{vac} ¹⁷. Let us write $\mathcal{F}(h)$ for the analytic function of h which coincides with \mathcal{F}_{vac} at *positive* real h . Then the analytic continuation of $\mathcal{F}(h)$ to the negative real values of h describes the energy density $\mathcal{F}_{\text{meta}}$ of the “false” vacuum – the Lorentz invariant metastable state having the magnetization opposite to the external field h (e.g. $\langle \sigma(x) \rangle_{\text{meta}} < 0$ at $h > 0$). It is natural to interpret the difference

$$\mathcal{F}_{\text{meta}} - \mathcal{F}_{\text{vac}} \quad (6.10)$$

as the effective string tension. Indeed, when the two quarks constituting a meson are widely separated (the configurations responsible for the singular terms in (6.7)),

¹⁶Although regular at $p \pm q = 0$, the term $\Delta \mathbb{G}_P^{(\text{reg})}(p|q)$ certainly has other singularities; even when p and q are real one expects to have branch cuts associated with the multi-particle thresholds.

¹⁷The vacuum energy density \mathcal{F}_{vac} is of course the same as the (singular part of) specific free energy of the near-critical Ising model.

the spatial domain between the quarks is effectively filled with the “false” vacuum. It follows that the coefficients in (6.8) are expressed through \tilde{g}_n as

$$c_{2k} = -2\tilde{g}_{2k+1} \quad (6.11)$$

This relation provides several terms in (6.8), since many coefficients in (6.9) are known¹⁸. In particular

$$c_2 = -0.003889\dots \quad (6.12)$$

The correction terms in (6.8) also make contributions to the low energy expansion (6.4). The first term affected is $\mu_8 t^8$,

$$\mu_8 = \epsilon_8 + \frac{2c_2 + a_2}{3} \epsilon_2. \quad (6.13)$$

Corrections to the terms $\sim t^9$ and higher involve additional contributions from the regular term in (6.7), see below.

It is tempting to take the difference (6.10) as the nonperturbative definition of the effective string tension f . It cannot be valid literally though. The function $\mathcal{F}(h)$ is known to have a branch cut along the negative part of the real axis [23], hence the analytic continuation defining $\mathcal{F}_{\text{meta}}$ in fact returns complex values. The imaginary part is interpreted in terms of the tunneling decay probability [24] and, being exponentially small in h , it is invisible in the perturbative expansion (6.8). In fact, both \mathcal{F}_{vac} and $\mathcal{F}_{\text{meta}}$ are known numerically with high precision, see Ref. [4]. In Fig.6 we show a plot of the difference (6.10) (measured in the units of $|h|^{\frac{16}{15}}$) as the function of the scaling parameter (1.2). One can see that the imaginary part of (6.10) is much smaller than the real part at all positive η (moreover, it essentially vanishes at $\eta \gtrsim 0.8$), therefore taking the real part seems to provide a reasonable definition for the effective string tension f . Note that the real part differs very little from the bare string tension f_0 at all but very small (positive) η . The difference is significant at $\eta \lesssim 0.8$, and becomes drastic at $\eta \rightarrow 0$. Indeed, at small η the bare tension tends to zero in a singular way, $f_0 \sim \eta^{\frac{1}{8}}$, while the difference (6.10) has finite limit at $\eta = 0$, and is analytic in some domain around this point. In fact, a number of terms of its Taylor expansion around $\eta = 0$ can be extracted from the results of [4]; for instance, for the real part f_{re} of (6.10) we have

$$f_{\text{re}} = |h|^{\frac{16}{15}} (\rho_0 + \rho_1 \eta + \rho_2 \eta^2 + \dots), \quad (6.14)$$

where the coefficients are expressed through Φ_k defined in Ref. [4] (see Table 3 there) as $\rho_k = (\cos \frac{8\pi(k-2)}{15} - 1) \Phi_k$, for instance

$$\rho_0 = 2.3692934\dots, \quad \rho_1 = 0.3521342\dots, \quad \rho_2 = 0, \quad \text{etc} \quad (6.15)$$

¹⁸The related coefficients $\tilde{G}_n = (2\bar{s})^n \tilde{g}_n$ are collected in Table 2 of the Ref. [4].

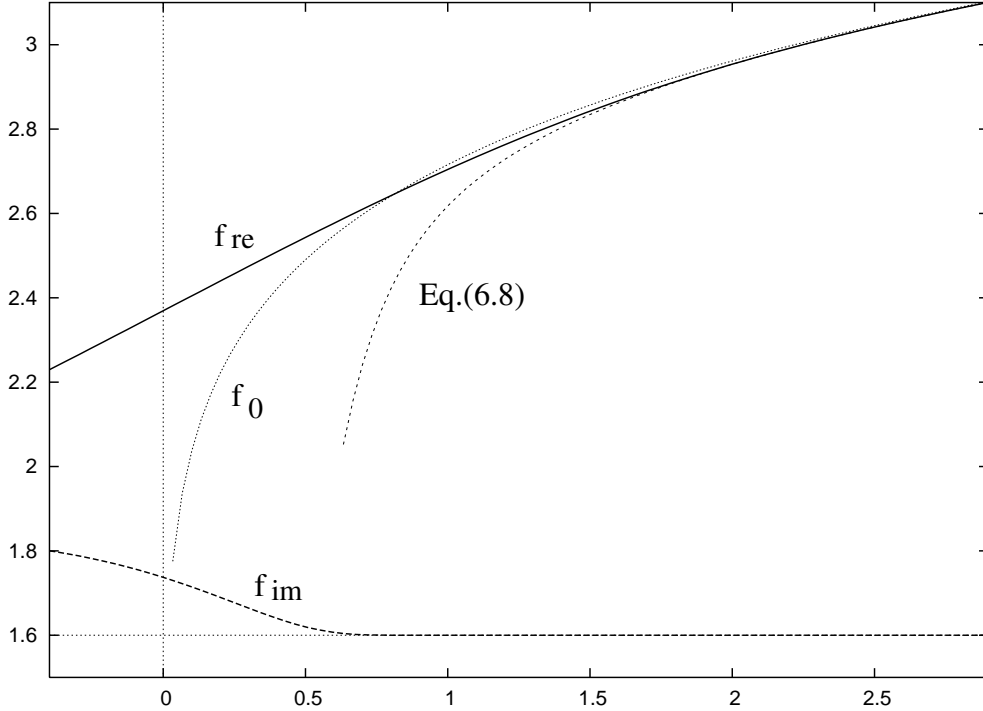


Figure 6: Plot of the difference (6.10) measured in the units of $|h|^{\frac{16}{15}}$, vs the scaling parameter η . The solid line and the “fat” dashed line represent the real and the imaginary parts $f_{\text{re}} = \Re[\mathcal{F}_{\text{meta}} - \mathcal{F}_{\text{vac}}]$ and $f_{\text{im}} = \Im m(\mathcal{F}_{\text{meta}} - \mathcal{F}_{\text{vac}})$, respectively. The imaginary part is shifted upward by 1.6 to make the Figure more compact. The dotted line represents the bare string tension $f_0 = (2\bar{s}\eta^{\frac{1}{8}})|h|^{\frac{16}{15}}$, and the fine dashed line shows the effect of the first correction to f_0 explicitly written in Eq.(6.8).

According to the above analysis, the singular parts of the multi-quark corrections in (6.1) modify the weak coupling expansions in a relatively trivial way, through the renormalizations of the parameters m and f_0 entering the BS equation (4.8), which are to be replaced by the “dressed” parameters m_q and f . Thus, the singular terms are taken into account by substituting

$$m \rightarrow m_q, \quad \lambda \rightarrow f/m_q^2 \quad (6.16)$$

in the low-energy expansion (5.16), and the same applies to the semiclassical expansion (5.26) as well. Remaining multi-quark corrections are associated with the regular term in (6.7). It is not difficult to show that this kind of corrections affects the low-energy expansion (6.4) only at the order t^9 and higher. Indeed, the term

$\Delta\mathbb{G}_P^{(reg)}(p|q)$ is regular at sufficiently small p and q , and it is an odd function of each of this variables. Therefore its leading low-energy behavior is

$$\Delta\mathbb{G}_P^{(reg)}(p|q) \rightarrow A(P) p q + \dots . \quad (6.17)$$

Since this term is there entirely due to the higher-order corrections, the coefficient $A(P)$ here is $\sim \lambda$. Recall also that the low-energy domain corresponds to $p, q \sim t$. It follows that the correction to the BS equation due to this regular term is $\sim t^9 = \lambda^3$. Similarly, one can check that the regular term leads to the corrections to the semi-classical quantization condition (5.26) at the order $\sim \lambda^3$ and higher. Therefore developing the weak coupling expansions (both the low-energy and the semiclassical ones) of the actual meson masses at the order λ^3 and beyond requires explicit evaluation of the contributions from the “regular” term $\Delta\mathbb{G}_P^{(reg)}$ in (6.7). The latter constitutes a separate and rather involved problem which we do not attempt to handle here. Note that the correction term $\sim \lambda^3$ to the quark mass in the Eq.(6.2), whose coefficient a_3 is also presently unknown, contributes at the same order. To summarize, existing data are sufficient to determine the coefficients of the weak coupling expansions of M_n all the way up to, but not including, the order λ^3 . Evaluating further terms requires additional ingredients, most importantly developing a perturbative expansion of the term $\Delta\mathbb{G}_P^{(reg)}$ and the higher-order corrections to the quark mass.

The above analysis, in particular the low-energy expansion, apply to stable mesons, with the masses M_n well below the stability threshold $2M_1$, twice the mass M_1 of the lightest meson. As given meson mass approaches to the threshold, one expects the threshold singularities of the last term in (6.7) to play more and more important role. As the result, when close to the threshold the actual mass M_n is expected to deviate significantly from its BS approximation \widetilde{M}_n . Furthermore, when the meson mass exceeds the threshold the actual mesons turn into resonances (see footnote⁶ on page 4), and their masses M_n develop imaginary parts representing the decay probabilities. This effect is certainly outside the scope of the two-quark approximation: the BS equation (4.8) describes an infinite tower of stable mesons. And even including the multi-quark states perturbatively, as was discussed above, does not seem to provide a consistent way of treating the mesons above the stability threshold. Let us mention interesting attempt to treat the issue of the unstable mesons on the perturbative level in Ref. [13]. However, we believe that systematic treatment of the decay problem must involve at least some understanding of the meson scattering states, the problem which we hope to address in the future.

7 Numerical solution

As we will argue in the next Section, the usefulness of the Bethe-Salpeter equation goes well beyond the derivation of the weak-coupling expansions (5.16), (5.26). Therefore it is of interest to study the eigenvalues \widetilde{M}_n^2 of the BS equations (4.11) at all values of λ , real and complex¹⁹. The equation (4.8) is unlikely to admit an analytic solution, but its numerical solution is not difficult to develop. The only feature which makes the numerical approach not exactly straightforward is the presence of the singularities of the kernel (4.9) at $\theta' = \pm\theta$. This is one of many features that the equation (4.8) shares with the mass spectrum equation in the 't Hooft's model [14]. Several methods have been developed for numerical solution of the latter (see [14,25]). We found it convenient to use yet another approach which is based on the Fourier-transformed version of the equation (4.8). We introduce the rapidity Fourier-transform

$$\Psi(\theta) = \int_{-\infty}^{\infty} \psi(\nu) e^{-i\nu\theta} d\nu, \quad \psi(\nu) = \int_{-\infty}^{\infty} \Psi(\theta) e^{i\nu\theta} \frac{d\theta}{2\pi}. \quad (7.1)$$

In terms of $\psi(\nu)$ the norm (4.10) becomes

$$\|\Psi\|^2 = \frac{1}{4} \int_{-\infty}^{\infty} \psi^*(\nu) K(\nu - \nu') \psi(\nu') d\nu d\nu', \quad (7.2)$$

where

$$K(\nu) = \int_{-\infty}^{\infty} \frac{e^{i\nu\theta}}{\cosh^2 \theta} \frac{d\theta}{2\pi} = \frac{\nu}{2 \sinh \frac{\pi\nu}{2}}, \quad (7.3)$$

and then the equation (4.8) transforms to

$$8 \left(m^2 + f_0 \nu \tanh \frac{\pi\nu}{2} \right) \psi(\nu) - \frac{f_0}{2} \frac{\nu}{\cosh \frac{\pi\nu}{2}} \int_{-\infty}^{\infty} \frac{\nu'}{\cosh \frac{\pi\nu'}{2}} \psi(\nu') d\nu' = M^2 \int_{-\infty}^{\infty} [K(\nu - \nu') - K(\nu + \nu')] \psi(\nu') d\nu' \quad (7.4)$$

Now the kernel is regular at any real arguments, and the equation (7.4) admits numerical solution through straightforward discretization of the variable ν . Before

¹⁹There are good reasons to expect that the BS masses \widetilde{M}_n , taken as the functions of complex λ (or rather of the complex variable $\bar{\eta} = 1/\sqrt{\lambda}$), imitate much of the analytic properties of the actual masses M_n in the complex η -plane. We will say more on this subject at the end of this Section, and again in Sect.9. In our view, gaining any insight into the analytic properties of $M_n(\eta)$ (structure of its Riemann surface, singularities, etc) is of central importance for overall understanding of IFT. This problem was one of primary motivations of our work.

turning to the numerics, let us say few words about the general properties of the BS equation written in this form.

It is not difficult to show that generic solution $\psi(\nu)$ has poles at the values of ν which solve the equation

$$1 + \lambda \nu \tanh \frac{\pi \nu}{2} = 0 . \quad (7.5)$$

where again $\lambda = f_0/m^2$. At real positive λ all solutions are purely imaginary, of the form $\pm i \kappa$, κ being a positive root of the equation

$$\lambda \kappa \tan \frac{\pi \kappa}{2} = 1 . \quad (7.6)$$

Let κ_0 be the lowest of such roots; at real positive λ it lays in the interval $[0, 1]$. The associated pole of $\psi(\nu)$ controls the large- θ behavior of the rapidity-space wave function,

$$\Psi(\theta) \rightarrow r \operatorname{sign}(\theta) e^{-\kappa_0 |\theta|} \quad \text{as } |\theta| \rightarrow \infty . \quad (7.7)$$

where r is a (normalization-dependent) constant. Note that at large λ this pole approaches the real axis, since

$$\kappa_0 \rightarrow \sqrt{\frac{2}{\pi \lambda}} \quad \text{as } \lambda \rightarrow \infty . \quad (7.8)$$

At $\lambda = \infty$ every eigenfunction $\psi_n(\nu)$ has a simple pole at $\nu = 0$; correspondingly, the associated rapidity wave function $\Psi_n(\theta)$ tends to a constant r_n at large $|\theta|$. One consequence of this phenomenon is the nature of the expansion around the point $\lambda = \infty$. This point appears to be a square-root branching point of the eigenvalues \widetilde{M}_n^2 taken as the functions of λ (see remark at the end of this Section). Therefore the large- λ expansions of \widetilde{M}_n^2 are of the form

$$\frac{\widetilde{M}_n^2}{4m^2} = Y_n^{(0)} \lambda + Y_n^{(1)} \sqrt{\lambda} + Y_n^{(2)} + \dots + Y_n^{(k)} \lambda^{1-\frac{k}{2}} + \dots , \quad (7.9)$$

where $Y_n^{(k)}$ are constants, and the series converge in finite domains. It is straightforward to derive the following expression for the coefficients at the terms $\sim \sqrt{\lambda}$,

$$Y_n^{(1)} = \frac{1}{2\sqrt{2\pi}} \left[\frac{|r_n|^2}{\|\Psi_n\|^2} \right]_{\lambda=\infty} , \quad (7.10)$$

where r_n are the constants in the asymptotics (7.7) of the wave functions Ψ_n .

n	$\lambda = 0.01$	$\lambda = 0.10$	$\lambda = 1.00$	$\lambda = 10.0$	$\lambda = 100$
1	1.110840242	1.550883388	4.185654285	24.29578962	205.1229687
2	1.196814699	2.024246733	7.637285443	56.34010255	523.5675928
3	1.269079423	2.446855032	10.96393850	88.01258645	838.4720639
4	1.334331298	2.845183371	14.23862629	119.5937889	1152.960249
5	1.395100728	3.228787972	17.48445168	151.1324905	1467.318135
6	1.452678928	3.602360894	20.71182429	182.6463568	1781.617148
7	1.507833369	3.968598364	23.92635268	214.1438592	2095.883687
8	1.561065333	4.329208970	27.13141319	245.6299865	2410.129928
9	1.612724086	4.685350869	30.32919948	277.1195629	2724.362364
10	1.663064726	5.037848886	33.52121875	308.8383150	3038.584826

Table 1: Ten lowest eigenvalues of the BS equation (4.11) at different values of λ obtained by numerical solution of the Eq.(7.4). The ratios $\widetilde{M}_n^2/4m^2$ are presented.

As was already said, numerical solution of (7.4) is obtained by discretization of the variable ν . In Table 1 we present few lowest eigenvalues \widetilde{M}_n^2 for some values of λ . At substantially smaller λ ($\lambda \leq 0.001$) the numerical results are indistinguishable (within the given accuracy) from the first eight terms of the low-energy expansion (5.16). On the other side, at large λ , the expansions (7.9) apply. Numerical estimates of the three leading coefficients Y for few lowest mesons are given in the Table 2. It is interesting to observe that as n grows the leading coefficients $Y_n^{(0)}$ quickly approach the following simple asymptotic form

$$Y_n^{(0)} \rightarrow \pi(n - 3/8) \quad \text{as } n \rightarrow \infty. \quad (7.11)$$

In the same limit $Y_n^{(1)}$ tend to a constant value 1.2533..., while $Y_n^{(2)}$ increases logarithmically as $\frac{1}{2} \log(n - 3/8) + \text{Const}$, with $\text{Const} \approx 1.209$.

Numerical diagonalization can be applied also at complex λ . The procedure is straightforward as long as $|\arg \lambda| < \pi$. But at $\arg \lambda = \pm \pi$ the poles $\nu = \pm i\kappa_0$ surface at the real ν -axis, and if one continues to the next sheet $|\arg \lambda| > \pi$ these poles break through the real axis, leaving behind the residue terms. Thus, at the second sheet one has to consider the equation which differs from the Eq.(7.4) by this residue term. Continuing around the point $\lambda = \infty$ second time generates another residue term which cancels exactly the first one. It follows that $\lambda = \infty$ is the square-root branching point of the solution, as was stated in the Eq.(7.9) above. Furthermore, one can argue that the BS masses \widetilde{M}_n , taken as the functions of complex λ exhibit infinitely many singularities on the second sheet of the λ -plane. Indeed, as was explained above, when continuing to the second sheet $\arg \lambda > \pi$,

n	$Y_n^{(0)}$	$Y_n^{(1)}$	$Y_n^{(2)}$	n	$Y_n^{(0)}$	$Y_n^{(1)}$	$Y_n^{(2)}$
1	1.904347602	1.3810744	0.873	6	17.67032120	1.25432903	2.072
2	5.094667187	1.2671521	1.450	7	20.81220388	1.25403891	2.154
3	8.242239347	1.2582803	1.691	8	23.95398627	1.25385735	2.224
4	11.38577501	1.2558373	1.853	9	27.09571021	1.25373628	2.286
5	14.52825003	1.2548349	1.974	10	30.23739767	1.25365155	2.341

Table 2: Three leading coefficients of the expansion (7.9) for the first ten eigenvalues \widetilde{M}_n^2 . The Eq.(7.10) was used in computing $Y_n^{(1)}$.

the pole at $\nu = i\kappa_0$ sinks into the lower half-plane, where at certain values of λ it collides with other poles of $\psi(\nu)$, associated with the higher roots of the equation (7.6). It is possible to show that these singularities accumulate towards the point $\lambda = 0$, making this point an essential singularity of all BS masses. This picture was behind our statement in Section 5 about the asymptotic nature of the weak coupling expansions. But detailed understanding of the analytic properties of the BS masses \widetilde{M}_n as the functions of complex λ remains to be achieved, and we intend to come back to this problem elsewhere.

8 Comparison to the TFFSA data

By construction, the BS equation was designed to describe stable mesons at sufficiently small λ , where the idea of the mesons as predominantly two-quark constructs is well justified. However, it turns out that this approximation describes the mass spectrum of stable mesons remarkably well for all but very large values of λ . Moreover, when some multi-quark effects (notably the renormalizations of the string tension) are taken into account, the approximation works very well at all real positive λ . In this Section we compare the results derived from the BS equation with the data on the mass spectrum obtained directly from the IFT using the TFFSA [4]. It is convenient in this context to discuss in terms of the scaling parameter (1.2) related to λ as

$$\lambda = \frac{2\bar{\sigma}h}{m^2} = \frac{2\bar{s}}{\eta^{\frac{15}{8}}}, \quad (8.1)$$

where \bar{s} is the constant defined in (2.2). In the following discussion we still reserve the notation M_n (or $M_n(\eta)$ when the dependence on η is to be emphasized) for the actual masses of the particles in the IFT, and use the notation \widetilde{M}_n for the BS

masses, obtained from the equation (4.8). In fact, we will often write $\widetilde{M}_n(m, f_0)$ to signify their dependence on the parameters in the Eq.(4.8).

We do not describe here the TFFSA in any details, which are presented in Ref. [4]. The strategy for extraction the particle masses is not much different from that commonly used in the TCSA [12]. We have employed additional improvements (mostly in the way the finite-size effects are taken into account) which will be described in due details in a separate paper. We have used this technique to determine the actual masses M_n of stable particles, at positive η ranging from 0 to 24. With the truncated space involving approximately 1800 lowest levels we were able to achieve typical accuracy of five significant digits for all those values of η , except for when the mass M_n is very close to the stability threshold $2M_1$, where the accuracy may be somewhat lower. The results were shown in Fig.1 for $\eta \in [-1 : 4]$ (at greater values of η deviations from the weak coupling approximations (5.16) or (5.26) would not be visible). Beyond the threshold $2M_1$ the particles become resonance states, their masses M_n acquiring imaginary parts²⁰. At $\eta = 0$ most of the resonances disappear, while some become stable particles again, in accord with the spectrum of the integrable IFT at $\eta = 0$. The masses at $\eta = 0$ are known exactly [5, 26], and TFFSA reproduces them within the stated accuracy. For all we know, the integrable point $\eta = 0$ is analytic, in particular the masses $M_n = M_n(\eta)$ admit power series expansions²¹

$$M_n(\eta) = M_n^{(0)} + M_n^{(1)} \eta + M_n^{(2)} \eta^2 + \dots . \quad (8.2)$$

The slopes $M_n^{(1)}$ for few lowest n are also known exactly, through the form-factor perturbation theory [6], and our TFFSA data is in full accord with the exact results (for previous numerical verification of the exact slopes using the lattice model see Ref. [27]). These numbers, as well as numerical estimates of the next term coefficients for the lowest mesons are collected in the Table 3.

As expected, at large η the masses from TFFSA agree very well with the low-energy expansions (6.4). This is demonstrated in Fig.7, where the differences $M_n(\eta) - \widetilde{M}_n(m, f_0)$ (with $\eta = (2\bar{s}m^2/f_0)^{8/15}$) for the three lowest mesons are shown at large $\eta > 10$. In this domain the BS masses $\widetilde{M}_n(m, f_0)$ are accurately described by the low-energy expansions (5.16). According to the arguments in Sect.6, the most part of the differences must be attributable to the quark mass renormalization (6.2),

²⁰It is possible to extract the masses and the widths of the resonances from the TFFSA data, and we have preliminary results for few lowest resonances. However, so far precision of our data is far from being satisfactory, especially when the resonances are wide, and we refrain from reporting this data here.

²¹Shifting away from the integrable point renders unstable all but the three lowest particles; correspondingly, the coefficients $M_n^{(2)}$ (and higher) with $n > 3$ generally have nonzero imaginary parts [6, 16].

n	$M_n^{(0)}$	$M_n^{(1)}$	$M_n^{(2)}$	$\widetilde{M}_n^{(0)}$	$\widetilde{M}_n^{(1)}$	$\widetilde{M}_n^{(2)}$
1	4.404908579981	1.295045	0.2003	4.248274145	1.316490	0.2815
2	7.127291799746	1.115886	0.2072	6.948600321	1.077762	0.3726
3	8.761556059774	1.953268	-1.5110	8.838163544	1.095065	0.3471
4	10.59322004129	1.484334	*****	10.387731645	1.144113	0.3212
5	13.02221009790	*****	*****	11.733999773	1.253651	*****

Table 3: The coefficients of the Taylor expansions (8.2) for four lowest mesons. The leading coefficients $M_n^{(0)}$ are exact masses of the integrable theory at $\eta = 0$ [5, 26]. The exact slopes $M_n^{(1)}$ are taken from Ref. [6], while the coefficients $M_n^{(2)}$ are estimated from the TFFSA data. The BS coefficients $\widetilde{M}_n^{(k)}$ are computed using (7.9) with $\lambda = f/m^2$, and the expansion (6.14) for f .

since its effect on the meson masses is $\sim \lambda^2$, while other multi-quark corrections are of higher orders. At large η the deviations look consistent with the asymptotic form $(a_2 \lambda^3) m = (4 a_2 \bar{s}^2 |h|^{8/15}) \eta^{-11/4}$ which corresponds to the leading quark mass correction (see Eq.(6.5)). The remaining mismatch visible in Fig.7 is likely to come from the unaccounted (and presently unknown) higher-order corrections to the quark mass, and perhaps from the multi-quark corrections to the regular part of the effective kernel discussed at the end of the Sect.6.

It turns out that even if all renormalization effects are disregarded, the BS masses $\widetilde{M}_n(m, f_0)$ approximate the actual masses \widetilde{M}_n very well at all but very small η . As is seen in the plot in Fig.8, the BS masses $\widetilde{M}_n(m, f_0)$ significantly deviate from M_n only at $\eta \lesssim 0.5$. Note that this is roughly the same region where the higher-order corrections to the string tension f become significant, see Fig.6. The dramatic drop of the BS masses $\widetilde{M}_n(m, f_0)$ at $\eta \rightarrow 0$ visible in the plot is certainly related to the singular behavior of f_0 in this limit. Therefore it is reasonable to expect that replacing f_0 with renormalized string tension f would take care of the most part of the mismatch at small η . As was already said, it is not completely clear how to determine the string tension f beyond the perturbation theory, but it is unlikely we can be off too far if we take, say, the real part of the difference (6.10), i.e. set

$$f = f_{\text{re}} \equiv \Re(\mathcal{F}_{\text{meta}} - \mathcal{F}_{\text{vac}}). \quad (8.3)$$

In particular, we recall that f_{re} has finite limit at $\eta = 0$, and in fact analytic around this point. As the result, the BS masses $\widetilde{M}_n(m, f_{\text{re}})$ are also analytic at $\eta = 0$, and their expansions around this point follow from (7.9) (where this time one sets $\lambda = f_{\text{re}}/m^2$), and (6.14). We show some coefficients of these expansions in Table 3, to compare with the coefficients in (8.2). To get further feeling of the matter, we

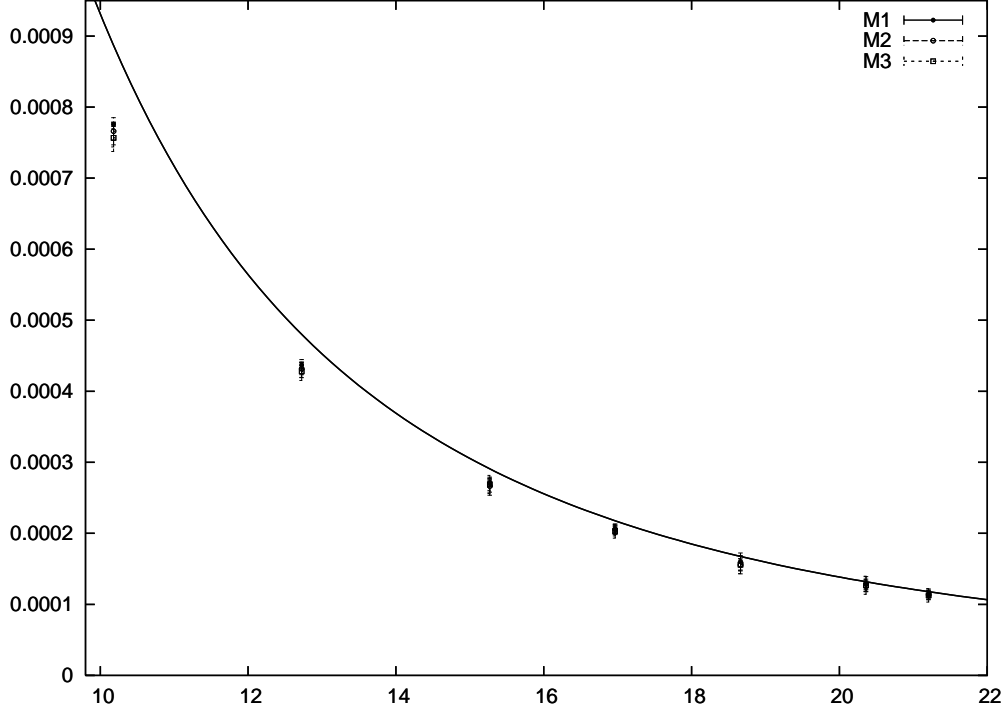


Figure 7: Plots of the differences $M_n - \widetilde{M}_n(m, f_0)$ (in the units of $|h|^{8/15}$), vs the scaling parameter η . The solid line is the curve $(4 a_2 \bar{s}^2) \eta^{-11/4}$ representing the correction $m a_2 t^6$ from the term a_2 in Eq.(6.5).

have computed numerically few lowest BS masses \widetilde{M}_n using f_{re} instead of f_0 in (4.8); the results (also shown in Fig.8) indeed come rather close to the actual masses at all positive η . It is tempting to attribute the remaining mismatch of the lowest BS masses $\widetilde{M}_n(m, f_{re})$ (clearly visible in Fig. 8 for $n = 1, 2, 3$) to the effect of the quark mass renormalization, so far disregarded. Indeed, if the correction to the quark mass is positive (as the λ^2 term in (6.2) is), its effect would be to shift the meson masses upward. Unfortunately, nothing is known about the higher-order corrections to m_q (other than the term (6.3), that is), let alone anything beyond the perturbative expansion. Just adding the known λ^2 term, while noticeably improving the BS masses at sufficiently large η (as was seen in Fig.7), leads to substantial overestimate of the actual masses at small η (Fig.8). This suggests that the properly defined m_q remains close to the bare quark mass m at all positive η , being perhaps no greater than $(0.1) |h|^{8/15}$ at $\eta = 0$.

Since the two-quark approximation can not account for the possible instability

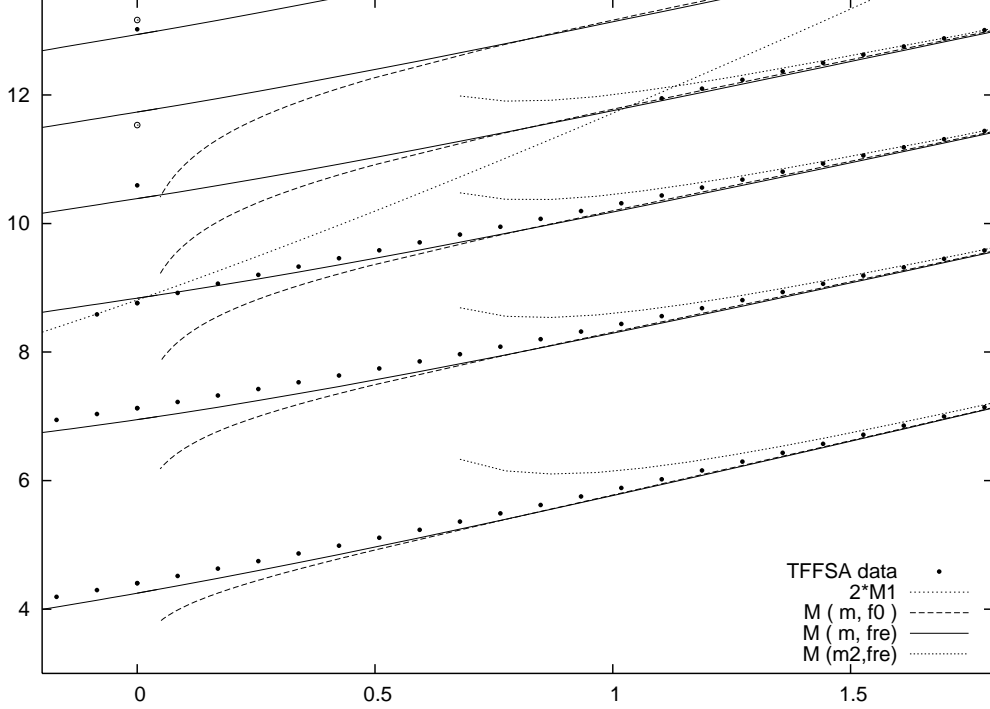


Figure 8: Plots of few lowest meson masses (in the units of $|h|^{\frac{16}{15}}$), vs the parameter η . The bullets \bullet represent the actual masses (exact values at $\eta = 0$, and the TFFSA data elsewhere. The uncertainties in the latter data are smaller than the size of the bullets). The fine dotted line is the stability threshold $2M_1$. The dashed lines are the masses $\widetilde{M}_n(m, f_0)$ from the BS equation with no renormalization effects taken into account. The solid lines are plots of $\widetilde{M}_n(m, f_{re})$. Effect of the first correction term in (6.2) is shown by the dotted lines. The circles \circ indicate position of the higher thresholds $M_1 + M_2$ and $M_1 + M_3$ at $\eta = 0$.

of the heavier mesons with respect to decays into the lighter ones, the BS masses \widetilde{M}_n remain real at all positive η . This is unlike the actual mesons which turn to resonances as soon as their masses cross the stability threshold $2M_1$. In fact the behavior of the actual masses $M_n(\eta)$ near the threshold is rather subtle (see footnote⁶ on page 4 for comment); this complex threshold behavior of the masses $M_3(\eta)$ and $M_4(\eta)$ is even visible in Fig.8. Of course this subtleties are not captured by the BS equation (4.8) - the BS masses \widetilde{M}_n go right through, without any anomalies at the threshold. This deficiency is the reason why in the Table 3, while $\widetilde{M}_3^{(0)}$ is rather close to $M_3^{(0)}$, the slope $\widetilde{M}_3^{(1)}$ and the curvature $\widetilde{M}_3^{(2)}$ are so much off - the point $\eta = 0$ is too close to the stability threshold $\eta_3 = -0.136(1)$ of the third particle. Let us

recall that it is when the meson mass approaches the threshold that the multi-quark corrections to the “regular” part of the BS kernel, Eq.(6.7), are expected to play a prominent role, and it is plausible that including such multi-quark corrections would help to understand better the threshold behavior.

In this paper we do not discuss the resonance part of the spectrum, putting this task away for another time. However let us make few remarks here. Although the BS equation (4.8) can not account for the instability of the mesons above the threshold (and thus disregards the imaginary parts of their masses), it likely captures the most of the real parts of the resonance masses. This is not inconsistent with the pattern readily observed in Fig.8. For example, the BS masses $\widetilde{M}_4(m, f_{re})$ and $\widetilde{M}_6(m, f_{re})$ at $\eta \rightarrow 0$ come reasonably close to the exact masses of the fourth and the fifth of the stable particles of the $\eta = 0$ theory, suggesting that analytic continuations of the actual masses $M_4(\eta)$ and $M_6(\eta)$ to the point $\eta = 0$ reproduce those exact masses. This rises a question about the fate of the mass $M_5(\eta)$ at $\eta \rightarrow 0$. Now, observe that the BS mass $M_5(m, f_{re})$ at $\eta \rightarrow 0$ lands far from $M_5^{(0)}$ (this is clearly seen in the last line of Table 3) but rather close to $M_1^{(0)} + M_2^{(0)}$, the sum of two lowest masses of the $\eta = 0$ theory. The most economic scenario then implies that for the actual masses we have $M_5(0) - M_1(0) - M_2(0) = 0$, and at $\eta \ll 1$ the state with mass $M_5(\eta)$ can be interpreted as a weakly coupled bound state of the two particles M_1 and M_2 . Of course it would be interesting to elaborate quantitative details of such scenario (and its versions for the higher resonances); again, we hope to address this problem in the future.

9 Discussion

In this paper we refine technique which allows for quantitative understanding of the mass spectrum of the IFT, in the low-T domain, in terms of “mesons” consisting predominantly of two quarks bound by a confining interaction. Thus we develop further the idea originally due to Wu and McCoy [3]. Systematic approach based on the idea of the mesons being essentially the two-quark constructs leads to the Bethe-Salpeter equation, Eq.(4.8), yielding a discrete spectrum of the meson masses. The Bethe-Salpeter equation is itself an approximation since it essentially ignores multi-quark components of the bound states. The approximation becomes exact in the weak field limit $\eta \rightarrow \infty$, but we show that it reproduces the masses of stable particles with reasonable accuracy at all positive η .

There is much room for further development. First, it seems to be possible (albeit involved) to take into account the multi-quark corrections perturbatively. This problem was briefly discussed in Section 6. It would be especially important to understand the role of the multi-quark corrections to the “regular” part of the BS

kernel, the term $\Delta\mathbb{G}_P^{(\text{reg})}$ in Eq.(6.7). That would help to get at least some insight into the way the meson masses behave near the stability threshold. Understanding of the above-threshold (i.e. resonance) part of the spectrum is another open problem (see however [13]).

As was mentioned in the Introduction, the main motivation of this work originated from our attempts to understand analytic properties of the IFT masses $M_n(\eta)$ as the functions of complex η . There are reasons to believe that at least some singularities of these functions are mimicked by the BS masses $\widetilde{M}_n(m, f)$, considered as the functions of complex variable $\bar{\eta} = m/\sqrt{f}$, and understanding analytic properties of the BS masses is a much more manageable problem. For instance, one type of singularities - those appearing due to collisions of the roots of the equation (7.5) - was mentioned at the end of Sect.7. These are square-root branching points, located somewhere at $|\arg \bar{\eta}| > 3\pi/4$ (We plan to discuss these singularities in more details elsewhere). It is likely that the actual IFT masses $M_n(\eta)$ have similar singularities at $|\arg \eta| > 11\pi/15$. Another question of much interest concerns locations of possible zeros of the BS masses \widetilde{M}_n on the Riemann surface of $\bar{\eta}$. At least some of such zeros may signal divergence of the correlation length in the full-fledged IFT, where one would expect to observe associated critical points. In this manner, vanishing of the lowest meson mass $M_1(\eta)$ at $\eta = (2.4295\dots) e^{\pm i\frac{11}{15}\pi}$ is related to the Yang-Lee edge singularity [4]. It is certainly interesting to contemplate the possibility that the Yang-Lee edge singularity is but one of many critical points one can bump into when wandering on the Riemann surface of η in the IFT. To some extent, the present paper can be regarded as a preparation to this analysis, and we hope to address this family of problems in future work.

Finally, some of the techniques developed here, in particular the weak coupling expansions in Sect.5, can be useful in other 2D theories which exhibit confinement of quarks, notably the 2D model of multicolor QCD (the 't Hooft model). More generally, there is a large class of systems having degeneracy of the ground state, which are integrable (with factorizable S-matrix of kinks), but not free. Typical perturbations of such theories lift the ground state degeneracy and creates confining force for the kinks. It seems important to extend the approach developed here to such systems.

Appendix

A Infinite-momentum limit of Eq.(3.11)

Here we derive the $P \rightarrow \infty$ limit of the equation (3.11). We assume that $\varepsilon(p)$ has exact asymptotic behavior (4.6), and that $\Delta E(P)$ has the form (4.5), in particular

$$\Delta E = |P| + \frac{M^2}{2|P|} + O(|P|^{-3}). \quad (\text{A.1})$$

Both sides of (3.11) can be expanded in inverse powers of P . Assume that $\Psi_P(p)$ is normalized in such a way that at $|p| < P/2$ it has finite nonzero limit as $P \rightarrow +\infty$. Under such normalization, $\Psi_P(p)$ with $|p| > P/2$ tends to zero as $P \rightarrow +\infty$. More precisely, if $u = 2p/P$ is fixed,

$$\Psi_P(p) = \begin{cases} O(1) & \text{at } |u| < 1 \\ O(P^{-2}) & \text{at } |u| > 1 \end{cases} \quad \text{as } P \rightarrow \infty. \quad (\text{A.2})$$

Indeed, consider the left-hand side of the equation (3.11). The coefficient in front of $\Psi_P(p)$ has different $P \rightarrow \infty$ behavior depending on whether $|u|$ is smaller or greater than 1, namely

$$\text{l.h.s. of (3.11)} \rightarrow \begin{cases} P^{-1} \left[\frac{2m^2}{1-u^2} - \frac{M^2}{2} \right] \Phi(u) & \text{at } |u| < 1 \\ P \left[|u| - 1 \right] \Phi(u) & \text{at } |u| > 1 \end{cases} \quad \text{as } P \rightarrow \infty, \quad (\text{A.3})$$

where

$$\Phi(u) = \lim_{P \rightarrow \infty} \Psi_P(uP/2). \quad (\text{A.4})$$

On the other hand, the kernel $G_P(p|q)$ decays as $1/P^2$ at all $p, q \sim P$, and hence the right-hand side of (3.11) is $\sim P^{-1}$ at all u . As the consequence, the limiting wave-function $\Phi(u)$, Eq.(A.4), must vanish outside the interval $|u| < 1$,

$$\Phi(u) = 0 \quad \text{at } |u| > 1. \quad (\text{A.5})$$

Comparing the $1/P$ terms in both sides of (3.11), we obtain the equation

$$\left[\frac{m^2}{1-u^2} - \frac{M^2}{4} \right] \Phi(u) = f_0 \int_{-1}^1 F(u|v) \Phi(v) \frac{dv}{2\pi}, \quad (\text{A.6})$$

where

$$F(u|v) = \frac{1}{\sqrt{(1-u^2)(1-v^2)}} \left[\frac{1-uv}{(u-v)^2} - \frac{1+uv}{(u+v)^2} + \frac{uv}{4} \right]. \quad (\text{A.7})$$

Changing variables $u = \tanh \theta$, $v = \tanh \theta'$ one arrives at (4.8) with $\Psi(\theta) = \Phi(\tanh \theta)$.

Note that the equation (A.6) is very similar to the Bethe-Salpeter equation determining the mass spectrum of mesons in the 't Hooft's model [14]. When the two quarks have equal masses the latter differs from (A.6) only in the detailed form of the kernel, which in that case is somewhat simpler,

$$F_{\text{'t Hooft}}(u|v) = \frac{1}{(u-v)^2} \quad (\text{A.8})$$

(also, the parameter f_0 is to be interpreted as the square of the gauge coupling constant).

B Derivation of the Eq.(5.5)

Here we evaluate the action of the operator $\hat{H} - M^2$ (with \hat{H} defined in (4.12)) on the wavefunction (5.2). It is useful to split the letter into two pieces,

$$\Psi_0(\theta) = \Psi_+(\theta) - \Psi_+(-\theta) , \quad (\text{B.1})$$

with

$$\Psi_+(\theta) = \frac{1}{2} \int_{-\infty}^{\infty} \frac{e^{i\lambda S(\beta)}}{\sinh(\theta + \beta - i0)} d\beta , \quad (\text{B.2})$$

and evaluate the corresponding two terms separately. In fact we need only to evaluate $[\hat{H} - M^2]\Psi_+(\theta)$; the desired result is then obtained by taking the part antisymmetric with respect to the reflection $\theta \rightarrow -\theta$. It will be also convenient to represent the operator $\hat{H} - M^2$ as the sum of two terms

$$[\hat{H} - M^2]\Psi(\theta) = 4m^2 \cosh^2 \theta [\hat{\Omega}\Psi(\theta) + \hat{G}\Psi(\theta)] , \quad (\text{B.3})$$

where

$$\hat{\Omega}\Psi(\theta) = \Omega(\theta)\Psi(\theta) , \quad \text{with} \quad \Omega(\theta) = -\frac{\partial}{\partial \theta} S(\theta) = 1 - \frac{M^2}{4m^2} \frac{1}{\cosh^2 \theta} , \quad (\text{B.4})$$

and

$$\hat{G}\Psi(\theta) = -\lambda \int_{-\infty}^{\infty} G_0(\theta - \theta') \Psi(\theta) \frac{d\theta'}{2\pi} + \frac{\lambda}{4} \frac{\sinh \theta}{\cosh^2 \theta} \bar{\Psi} . \quad (\text{B.5})$$

In the last equation we have introduced the notations

$$G_0(\theta - \theta') = 2 \frac{\cosh(\theta - \theta')}{\sinh^2(\theta - \theta')} , \quad \bar{\Psi} = \int_{-\infty}^{\infty} \frac{\sinh \theta}{\cosh^2 \theta} \Psi(\theta) \frac{d\theta}{2\pi} . \quad (\text{B.6})$$

Let us first transform the integral

$$\begin{aligned}
-\lambda \int_{-\infty}^{\infty} G_0(\theta - \theta') \Psi_+(\theta') \frac{d\theta'}{2\pi} = & \quad (B.7) \\
\frac{d}{d\theta} \int_{-\infty}^{\infty} \frac{\lambda}{\sinh(\theta - \theta')} \frac{d\theta'}{2\pi} \int_{-\infty}^{\infty} \frac{e^{\frac{i}{\lambda} S(\beta)} d\beta}{\sinh(\theta' - \beta - i0)}. &
\end{aligned}$$

The order of integrations can be interchanged, and at fixed real β the contour of integration over θ' can be shifted downward, $\theta' = \alpha - i\pi/2$; this leaves behind half of the residue at the pole $\theta' = \theta$,

$$(B.8) = \frac{i}{2} \int_{-\infty}^{\infty} \frac{\partial}{\partial \theta} \frac{\lambda e^{\frac{i}{\lambda} S(\beta)} d\beta}{\sinh(\theta + \beta - i0)} + \frac{d}{d\theta} \int_{-\infty}^{\infty} \frac{d\beta}{2\pi} \int_{-\infty}^{\infty} \frac{\lambda e^{\frac{i}{\lambda} S(\beta)} d\alpha}{\cosh(\theta - \alpha) \cosh(\alpha + \beta)}.$$

In the first term we transfer the derivation over θ to the integration variable β , and then integrate by parts. The integral over α in the second term is evaluated in closed form. One finds

$$(B.8) = -\frac{1}{2} \int_{-\infty}^{\infty} \frac{\Omega(\beta) e^{\frac{i}{\lambda} S(\beta)} d\beta}{\sinh(\theta + \beta - i0)} + \frac{\lambda}{\pi} \int_{-\infty}^{\infty} \left[\frac{\partial}{\partial \beta} \frac{\theta + \beta}{\sinh(\theta + \beta)} \right] e^{\frac{i}{\lambda} S(\beta)} d\beta, \quad (B.8)$$

where the factor $-\Omega(\beta)$ in the first term came from the derivative of $S(\beta)$, see Eq.(B.4). Note that when plugged into (B.3), the first term combines nicely with the term $\Omega(\theta)\Psi_+(\theta)$, to produce

$$\int_{-\infty}^{\infty} \frac{1}{2} \frac{\Omega(\theta) - \Omega(\beta)}{\sinh(\theta + \beta - i0)} e^{\frac{i}{\lambda} S(\beta)} d\beta. \quad (B.9)$$

Since the numerator in the integrand vanishes at $\beta = -\theta$, this point is no longer singular, and the shift $-i0$ in the denominator is irrelevant. In fact, the integrand in (B.9) can be reduced to

$$\frac{M^2}{8m^2} \frac{\sinh(\theta - \beta)}{\cosh^2 \theta \cosh^2 \beta} e^{\frac{i}{\lambda} S(\beta)}. \quad (B.10)$$

Next, when applied to Ψ_+ , the second term in right-hand side of (B.5) involves the factor

$$\begin{aligned}
\bar{\Psi}_+ = \frac{1}{2} \int_{-\infty}^{\infty} \frac{\sinh \theta}{\cosh^2 \theta} \frac{d\theta}{2\pi} \int_{-\infty}^{\infty} \frac{e^{\frac{i}{\lambda} S(\beta)}}{\sinh(\theta + \beta - i0)} d\beta = & \\
\int_{-\infty}^{\infty} \left[\frac{i}{4} \frac{\sinh \beta}{\cosh^2 \beta} - \frac{1}{2\pi} \frac{\partial}{\partial \beta} \frac{\beta}{\cosh \beta} \right] e^{\frac{i}{\lambda} S(\beta)} d\beta, & \quad (B.11)
\end{aligned}$$

where the expression in the second line results from explicit evaluation of the integral over θ .

Putting the Eq's. (B.4), (B.5), (B.8), and (B.11) together, we find

$$[\hat{\Omega} + \hat{G}] \Psi_+(\theta) = \int_{-\infty}^{\infty} \left[\frac{M^2}{8m^2} \frac{\sinh(\theta - \beta)}{\cosh^2 \theta \cosh^2 \beta} + \frac{\lambda}{\pi} \frac{\partial}{\partial \beta} \left(\frac{\theta + \beta}{\sinh(\theta + \beta)} - \frac{1}{8} \frac{\sinh \theta}{\cosh^2 \theta} \frac{i\pi/2 + \beta}{\cosh \beta} \right) \right] e^{\frac{i}{\lambda} S(\beta)} d\beta. \quad (\text{B.12})$$

Finally, isolating the odd part of this expression, one arrives at (5.5).

Acknowledgments

One of us (AZ) is pleased to acknowledge kind hospitality extended to him at the Institute of Physics of the University of Bonn, and at the Ecole Normale Supérieure, where parts of this work was done. Supports from the Alexander von Humboldt Foundation, and Blaise Pascal Research Chair, which made these visits possible, are gratefully appreciated. We would like to express gratitude to Alyocha Zamolodchikov, Sergei Lukyanov, and Volodya Fateev for many stimulating discussions and helpful remarks. AZ also benefited a lot from conversations with Vladimir Bazhanov, Vladimir Kazakov, and Vladimir Rittenberg. Research of AZ is supported by DOE grant # DE-FG02-96ER40949.

References

- [1] C. Itzykson, J.-M. Drouffe, *Statistical field theory*, Cambridge University Press, 1989.
- [2] P. Di Francesco, P. Mathieu, D. Sénéchal, *Conformal Field Theory*, Springer, 1996
- [3] B.M. McCoy, T.T. Wu, *Two-dimensional Ising field theory in a magnetic field: breakup of the cut in the two-point function*, Phys. Rev. D 18 (1978) 1259–1267.
- [4] P. Fonseca, A. Zamolodchikov, *Ising field theory in a magnetic field: analytic properties of the free energy*, J. Stat. Phys. 110 (2003) 527–590, hep-th/0112167
- [5] A.B. Zamolodchikov *Integrals of motion and S matrix of the (scaled) $T = T_c$ Ising model with magnetic field.*, Int.J.Mod.Phys. A4 (1989) 4235, *Integrable field theory from conformal field theory*, Advanced Studies in Pure Mathematics 19 (1989) 641-674

- [6] G. Delfino, G. Mussardo, P. Simonetti, *Non-integrable quantum field theories as perturbations of certain integrable models*, Nucl. Phys. B 473 (1996) 469–508; hep-th/9603011.
- [7] T.T. Wu, B.M. McCoy, *The two-dimensional Ising model*, Harvard University Press, 1973.
- [8] C.N. Yang, T.D. Lee, *Statistical Theory of Equation of State and Phase Transitions. I. Theory of Condensation*, Phys.Rev. 87 (1952) 404-409; T.D. Lee, C.N. Yang, *Statistical Theory of Equation of State and Phase Transitions. II. Lattice Gas and Ising Model*, Phys.Rev. 87 (1952) 410-419.
- [9] M.E. Fisher, *Yang-Lee Edge Singularity and φ^3 Field Theory*, Phys.Rev.Lett. 40, (1978) 1610-1613.
- [10] J.L. Cardy, *Conformal Invariance and the Yang-Lee Edge Singularity in Two Dimensions*, Phys.Rev.Lett. 54 (1985) 1354-1356.
- [11] J.L. Cardy, G. Mussardo, *S-Matrix of the Yang-Lee Edge Singularity in Two Dimensions*, Phys.Lett. B225 (1989) 275-278.
- [12] V.P. Yurov, Al.B. Zamolodchikov, *Truncated Conformal Space Approach to Scaling Lee Yang Model*, Int.J.Mod.Phys. A5 (1990) 3221-3245; V.P. Yurov, Al.B. Zamolodchikov, *Truncated Fermionic Space Approach to the Critical 2D Ising Model with Magnetic Field*, Int.J.Mod.Phys. A6 (1991) 4557-4578.
- [13] S.B. Rutkevich, *Large- N excitations in the ferromagnetic Ising field theory in a small magnetic field: mass spectrum and decay widths*, Phys.Rev.Lett. 95 (2005) 250601; hep-th/0509149
- [14] G. 't Hooft, *A two-dimensional model for mesons*, Nucl.Phys. B 75 (1974) 461–470
- [15] L.D. Landau and E.M. Lifshitz, *Quantum Mechanics (Non-relativistic Theory)*, Pergamon Press, 1991
- [16] G. Delfino, P. Grinza, G. Mussardo, *Decay of particles above threshold in the Ising field theory with magnetic field*, Nucl.Phys. B737 (2006) 291-303; hep-th/0507133
- [17] T.T. Wu, B.M. McCoy, C.A. Tracy, E. Barouch, *Spin-spin correlation functions for the two-dimensional Ising model: exact theory in the scaling region*, Phys. Rev. B 13 (1976) 316–374.

- [18] B. Berg, M. Karowski, P. Weisz, *Construction Of Green Functions From An Exact S Matrix*, Phys.Rev. D19 (1979).
- [19] C. Itzykson, J.-B. Zuber, *Quantum Field Theory*, McGraw-Hill, 1980.
- [20] I.Bars, M.B. Green, *Poincaré- and gauge -invariant two-dimensional quantum chromodynamics*, Phys. Rev. D 17, (1978), 537–545
- [21] B.M. McCoy, T.T. Wu, *Two-dimensional Ising model near T_c : Approximation for small magnetic field*, Phys.Rev. B18 (1978) 4886-4901.
- [22] P. Fonseca, A. Zamolodchikov, *Ward identities and integrable differential equations in the Ising field theory*, RUNHETC-2003-28, Sep 2003; hep-th/0309228
- [23] A.F. Andreev, *Singularity of Thermodynamic Quantities at a First Order Phase Transition Point*, JETP 18 (1964) 1415-1416; M.E. Fisher, University of Colorado Summer School Lectures, Boulder, 1964; J.S. Langer, *Theory of Condensation Point*, Ann.Phys.41 (1967) 108-157.
- [24] Voloshin, I.Yu. Kobzarev, L.B. Okun, M.B. Voloshin, *Bubbles in metastable vacuum*, Sov.J.Nucl.Phys. 20 (1975) 644-646; S. Coleman, *Fate of the false vacuum: Semiclassical theory*, Phys.Rev. D15 (1977) 2929-2936.
- [25] W. Krauth, M. Staudacher, *Nonintegrability of two-dimensional QCD*, Phys.Lett. B 388 (1996) 808–812; hep-th/9608122
- [26] V.A. Fateev, *The exact relations between the coupling constants and the masses of particles for the integrable perturbed Conformal Field Theories*, Phys.Lett. B 324 (1994) 45-51.
- [27] P. Grinza, A. Rago, *Study of the 2-D Ising model with mixed perturbation*, Nucl.Phys.B651 (2003), 387-412; hep-th/0208016
- [28] C.G. Callan, N. Coote, D.J. Gross, *Two-dimensional Yang-Mills theory: A model of quark confinement*, Phys.Rev. D13 (1976) 1649-1669.
- [29] G. Delfino, *Integrable field theory and critical phenomena: The Ising model in a magnetic field*, J.Phys. A37 (2004) R45.
- [30] M. Caselle, P.Grinza, A. Rago, *Amplitude ratios for the mass spectrum of the 2d Ising model in the high- T , $H \neq 0$ phase*, J.Stat.Mech. 0410 (2004), P009, e-Print Archive: hep-lat/0408044.